

CFD ANALYSIS OF AIR INTAKE SYSTEM OF 1.6L PROTON WAJA  
ENGINE BY ADDING GUIDE VANES

VIJAYAKUMAR A/L MARIMUTHU

BACHELOR OF ENGINEERING  
UNIVERSITI MALAYSIA PAHANG

2010

# UNIVERSITI MALAYSIA PAHANG

## BORANG PENGESAHAN STATUS TESIS

JUDUL: **CFD ANALYSIS OF AIR INTAKE SYSTEM OF 1.6L  
PROTON WAJA ENGINE BY ADDING GUIDE VANES**

SESI PENGAJIAN: 2010/2011

Saya VIJAYAKUMAR A/L MARIMUTHU(860805-38-5455)  
(HURUF BESAR)

mengaku membenarkan tesis (Sarjana Muda/~~Sarjana~~ /~~Doktor Falsafah~~)\* ini disimpan di Perpustakaan dengan syarat-syarat kegunaan seperti berikut:

1. Tesis adalah hakmilik Universiti Malaysia Pahang (UMP).
2. Perpustakaan dibenarkan membuat salinan untuk tujuan pengajian sahaja.
3. Perpustakaan dibenarkan membuat salinan tesis ini sebagai bahan pertukaran antara institusi pengajian tinggi.
4. \*\*Sila tandakan ( ✓ )

**SULIT**

(Mengandungi maklumat yang berdarjah keselamatan atau kepentingan Malaysia seperti yang termaktub di dalam AKTA RAHSIA RASMI 1972)

**TERHAD**

(Mengandungi maklumat TERHAD yang telah ditentukan oleh organisasi/badan di mana penyelidikan dijalankan)

**TIDAK TERHAD**

Disahkan oleh:

\_\_\_\_\_  
(TANDATANGAN PENULIS)

\_\_\_\_\_  
(TANDATANGAN PENYELIA)

Alamat Tetap:

**16, PERSIARAN RISHAH (S) 1/5,  
TAMAN BUNTONG RIA,  
30100 IPOH,  
PERAK DARUL RIDZUAN.**

Nama Penyelia:

**MUHAMMAD AMMAR BIN NIK  
MUTASIM**

Tarikh: **06 DECEMBER 2010**

Tarikh: **06 DECEMBER 2010**

CATATAN:\*  
\*\*

Potong yang tidak berkenaan.  
Jika tesis ini SULIT atau TERHAD, sila lampirkan surat daripada pihak berkuasa/organisasi berkenaan dengan menyatakan sekali tempoh tesis ini perlu dikelaskan sebagai atau TERHAD.  
Tesis dimaksudkan sebagai tesis bagi Ijazah doktor Falsafah dan Sarjana secara Penyelidikan, atau disertasi bagi pengajian secara kerja kursus dan penyelidikan, atau Laporan Projek Sarjana Muda (PSM).

CFD ANALYSIS OF AIR INTAKE SYSTEM OF 1.6L PROTON WAJA ENGINE BY  
ADDING GUIDE VANES

VIJAYAKUMAR A/L MARIMUTHU

Thesis submitted in partial fulfillment of the requirements  
for the award of the degree of  
Bachelor of Mechanical Engineering with Automotive Engineering

Faculty of Mechanical Engineering  
UNIVERSITI MALAYSIA PAHANG

DECEMBER 2010

**UNIVERSITI MALAYSIA PAHANG**  
**FACULTY OF MECHANICAL ENGINEERING**

We certify that the project entitled “CFD Analysis of Air Intake System Of 1.6L Proton Waja Engine by Adding Guide Vanes” is written by Vijayakumar A/L Marimuthu. We have examined the final copy of this project and in our opinion; it is fully adequate in terms of scope and quality for the award of the degree of Bachelor of Engineering. We herewith recommend that it be accepted in partial fulfillment of the requirements for the degree of Bachelor of Mechanical Engineering with Automotive Engineering.

MOHD. YUSOF TAIB

Examiner

Signature

### **SUPERVISOR'S DECLARATION**

“I hereby declare that I have read this thesis and in my opinion this thesis sufficient in terms of scope and quality for the award the degree of Bachelor of Mechanical Engineering with Automotive Engineering”

Signature : .....

Name of Supervisor : MUHAMMAD AMMAR BIN NIK MUTASIM

Position : LECTURER

Date : 06 DECEMBER 2010

### **STUDENT'S DECLARATION**

I declare that this thesis entitled Design Optimization Air Intake System of Proton Waja by Adding Guide Vane is the result of my own research except as cited in the references. The thesis has not been accepted for any degree and is not concurrently submitted in candidature of any other degree.

Signature : .....

Name of Candidate : VIJAYAKUMAR A/L MARIMUTHU

ID Number : MH 07051

Date : 06 DECEMBER 2010

*This work is dedicated to my beloved ones,  
My Father Mr. Marimuthu A/L Krishnan  
My Mother Mrs. Kanagi A/P Letchumanan  
My Brother Subramanium A/L Marimuthu  
My Sisters Ms. Thangam A/P Marimuthu*

*And*

*Allies...*

*Thank you for the endless support and encouragement.*

*You all always have a special place in my heart.*

## **ACKNOWLEDGEMENT**

I would like to express my deepest appreciation and gratitude to my supervisor, Mr. Muhammad Ammar Bin Nik Mustasim for his guidance, patience for giving advises and supports throughout the progress of this project. Special thanks are also given to all lecturers and vocational trainers for the guidance, experience sharing and comment on my project thesis. They were not hesitant to answer all my doubts and spending their time to guide me during my experimental work.

A great appreciation is acknowledged to the Faculty of Mechanical Engineering for the funding under the final year project.

Last but not least, I would like to thank all my friends for their support and encouragement given to me, especially during the hard times.



## ABSTRACT

The objective of the current research was to analyze the flow through the air intake system of 1.6L Proton Waja engine by adding guide vane. The pressure drop across the air intake system is known to have a significant influence on the indicated power of the SI engine. The pressure drop along the intake system is proportional to the engine speed and cross sectional area. The guide vane is placed in the system to reduce the pressure drop across the system. It was found that the guide vane help to reduce pressure drop across the air intake system where it increases the capabilities of air induction system to suck more air to the engine. The geometry of air intake system of Proton Waja 1.6L engine was used in the modeling approach. The study was focused on different engine speed. This analysis was done in CFD using a model setup with appropriate speed of the Proton Waja 1.6L engine from maximum speed to minimum speed. The CFD results of air intake system with the guide vane are validated against the CFD result of real air intake system of Proton Waja 1.6L which do not have guide vane.

## **ABSRTAK**

Tujuan kertas kajian ini adalah untuk menganalisis sistem penyerapan udara bagi kereta Proton Waja 1.6L enjin dengan menambah “guide vane”. Penurunan tekanan pada sistem “intake” mempunyai signifikan pada kuasa enjin SI. Penurunan tekanan sepanjang sistem penyerapan udara berkadar langsung dengan kelajuan enjin dan luas permukaan. “Guide vane” ditempatkan dalam sistem udara untuk mengurangkan penurunan tekanan di seluruh sistem penyerapan udara. Didapati bahawa dengan adanya “guide vane” ia membantu mengurangkan penurunan tekanan di seluruh sistem di mana ia juga secara langsung akan meningkatkan kemampuan sistem penyerapan untuk menyerap lebih banyak udara ke dalam enjin. Geometri sistem penyerapan udara bagi kereta Proton Waja 1.6L enjin telah digunakan dalam pendekatan pemodelan. Penelitian ini difokuskan pada kelajuan enjin yang berbeza. Analisis ini dilakukan dalam CFD dengan menggunakan setum model dengan kelajuan yang sesuai dari kelajuan minimum ke kelajuan maksimum. Keputusan CFD sistem penyerapan udara dengan “guide vane” diaktifkan terhadap hasil CFD sistem penyerapan udara tanpa “guide vane”.

## TABLE OF CONTENTS

	<b>Page</b>
<b>TITLE</b>	i
<b>EXAMINER’S DECLARATION</b>	ii
<b>SUPERVISOR’S DECLARATION</b>	iii
<b>STUDENT’S DECLARATION</b>	iv
<b>DEDICATION</b>	v
<b>ACKNOWLEDGEMENT</b>	vi
<b>ABSTRACT</b>	vii
<b>ABSTRAK</b>	viii
<b>TABLE OF CONTENTS</b>	ix
<b>LIST OF TABLES</b>	xii
<b>LIST OF FIGURES</b>	xiii
<b>LIST OF SYMBOLS</b>	xiv
<b>LIST OF ABBERVATION</b>	xv
<b>LIST OF APPENDICES</b>	xvi
<b>CHAPTER 1</b>	<b>INTRODUCTION</b>
	1.1 Project Background 1
	1.2 Problem Statement 2
	1.3 Project Objectives 3
	1.4 Scopes of Study 3
<b>CHAPTER 2</b>	<b>LITERATURE REVIEW</b>
	2.1 Air Intake System 4
	2.2 Helix Shape 5
	2.3 Swirls 6
	2.3.1 Low Swirl 7
	2.3.2 High Swirl 8
	2.3.3 Generation Of Swirl Flow 9
	2.3.4 Tangential Entry 9

2.3.5	Guide Vanes	10
2.3.6	Direct Rotation	12
2.4	Flow Rates In Horizontal Pipes	13
2.5	Pressure Drop And Head Los In A Pipe	14
2.6	Governing Equation	15
2.7	Reynolds Number Effect	15
2.7.1	Major Losess	17
2.7.2	Minor Losess	17
2.8	Mass And Volume Flow Rate	18
2.9	Air Flow Rate Required By The Engine	19

### **CHAPTER 3            METHODOLOGY**

3.1	Geometry of AIS and Simplification on It	21
3.2	Measurement and Modelling	22
3.3	3-D Modeling Software	22
3.4	Solid Works Model	23
3.5	CFD Condition	24
3.5.1	Computational Fluid Dynamics Simulation	24
3.5.2	CFD Simulation of The AIS	25
3.6	Air Properties	26
3.7	Specifications Of Proton Waja 1.6l (2000)	27
3.8	Calculation And Equations	28
3.8.1	Required Engine Air Flow Rate	28
3.8.2	Pressure Drop	28
3.8.3	Pressure Drop Improvement	29

### **CHAPTER 4            RESULT AND DISCUSSION**

4.1	Introduction	30
4.2	Pressure Drop and Velocity Difference	
	Table For Without Guide Vane AIS	32
4.3	Pressure Drop and Velocity Difference	
	Analysis Table For With Guide Vane AIS	33
4.4	Graphical Analysis Data Result	34
4.5	Results and Calculation	37

<b>CHAPTER 5</b>	<b>CONCLUSION AND RECOMMENDATION</b>	
5.1	Conclusion	41
5.2	Recommendation	42
<b>REFERENCES</b>		43
<b>APEENDICES</b>		
A	Moody Diagram	44
B	Pressure Distribution (Without Guide Vane) At Various Engine Speed	45
C	Pressure Distribution (With Guide Vane) At Various Engine Speed	47
D	Velocity Distribution (Without Guide Vane) At Various Engine Speed	49
E	Velocity Distribution (With Guide Vane) At Various Engine Speed	51

**LIST OF TABLES**

<b>TABLE NO.</b>	<b>TITLE</b>	<b>PAGE</b>
3.1	Properties of air	27
3.2	Specification of Proton Waja 1.6L (2000)	27
4.1	Pressure Drop for without guide vane	32
4.2	Velocity Increment for without guide vane	32
4.3	Pressure Drop for with guide vane	33
4.4	Velocity Increment for with guide vane	34
4.5	Engine air flow rate calculation	38
4.6	Pressure drop across AIS for with and without guide vane	39
4.7	Percentage improvement in total pressure drop	40

## LIST OF FIGURES

FIGURE NO.	TITLE	PAGES
2.1	Jet flow with low degree of swirl	7
2.2	Jet flow of high degree of swirl	8
2.3	Swirl generator	10
2.4	Moving block swirl burner	10
2.5	Double concentric swirl burner	11
2.6	Vane-type swirler in an axial tube flow	11
2.7	Rotating burner setup	12
2.8	Rotating screen for fire whirl experiment	13
2.9	Flow in the horizontal pipe	14
2.10	Transition between laminar and turbulent flow	16
2.11	Difference between with and without guide vane	18
3.1	Methodology	20
3.2	AIS located under the bonnet	21
3.3	AIS of Proton Waja 1.6L (2000)	23
3.4	AIS of Proton Waja 1.6L (2000) from different angles	24
3.5	AIS of Proton Waja 1.6L (2000)	28
4.1	Guide Vane placement on the down box	31
4.2	Guide Vane placement on the outlet pipe.	31
4.3	Pressure drop vs. engine speed	35
4.4	Velocity improvement vs. engine speed	35
4.5	Intake velocity vs. engine speed	36
4.6	Outlet velocity vs. engine speed	36

## LIST OF SYMBOLS

$A_1$	Area in inlet	$m^2$
$A_2$	Area at throat	$m^2$
D or L	lateral dimension of the body	m
$D_i$	Engine displacement	$m^3$
$H_L$	Losses in pipe	Pa
$\dot{m}$	Inlet mass flow rate	kg/s
N	Engine speed	rpm
$\eta_v$	Engine volumetric efficiency	-
U $\infty$	Air velocity	m/s
$\Delta p\%$	Improvement Pressure drop	-
$\Delta p$	Pressure drop	Pa
$\rho$	Air density at inlet	kg/m <sup>3</sup>
$V_a$	Engine air flowrate	m <sup>3</sup> /sec
$v_1$	Velocity at inlet	m/s
$v_2$	Velocity at throat	m/s
$\nu$	Kinematics viscosity	m <sup>2</sup> /s
$\mu$	Dynamic viscosity	kg/ms
$\gamma$	Specific Weight	N/m <sup>3</sup>



**LIST OF ABBREVIATIONS**

AIS	Air Intake System
CFD	Computational Fluid Dynamics

**LIST OF APPENDICES**

<b>APPENDIX</b>	<b>TITLE</b>	<b>PAGES</b>
A	Moody Diagram	42
B	Pressure Distribution (Without Guide Vane) At Various Engine Speed	43-44
C	Pressure Distribution (With Guide Vane) At Various Engine Speed	45-46
D	Velocity Distribution (Without Guide Vane) At Various Engine Speed	47-48
E	Velocity Distribution (With Guide Vane) At Various Engine Speed	49-50

## **CHAPTER 1**

### **INTRODUCTION**

#### **1.1 PROJECT BACKGROUND**

An internal combustion engine (ICE) is a heat engine in which the chemical energy in a fuel is released through combustion in the engine cylinder. This chemical energy will convert into mechanical energy, usually made available on a rotating shaft. Chemical energy of the fuel is first converted to thermal energy by means of combustion or oxidation with air inside the engine. This thermal energy raises the temperature and pressure of the gases within the engine and the high pressure gas then expands against the mechanical mechanisms of the engine. This expansion is converted by the mechanical linkages of the engine to a rotating crankshaft, which is output of the engine (W.W.Pulkrabek , 1993).

The combustion process required oxygen from the ambient through intake system during the intake stroke to bond with petrol (carbon and hydrogen). In order for the engine to be as efficient as possible it is required for the air to be mixed well with the petrol (bond of carbon and hydrogen), a well mixed of oxygen and petrol will improve the combustion. However the air motion in intake system will influence the combustion process. Understanding of flows and pressure drop through the system is essential to optimize the use of petrol (bond of carbon and hydrogen) in the combustion cylinder (May, 2003).

The physical aspects of any fluid flow are governed by the three fundamental principles that are conservation of mass, Newton's second law and conservation of energy. These fundamental principles can be expressed in terms of mathematical

equations, which in their most general form usually partial differential equations. Computational Fluid Dynamics (CFD) is the art of replacing the governing partial differential of fluid flow with numbers and advancing these numbers in space and time to obtain the final numerical description of the complete flow field of interest (J.D.Anderson, 2009). CFD is considered to be the most cost effective solution for flow analysis of intake system along the air intake system. This study is only focuses on the air motion behavior of the 1.6L engine Proton Waja air intake system and, with and without the swirl element placement on the air intake system just after the filter box and just before intake manifold by CFD analysis results.

## **1.2 PROBLEM STATEMENT**

For an internal combustion engine (ICE) the most suitable ratio of air to fuel is approximately 14.7:1 by mass, that is 14.7kg of air is required to combust with 1kg of petrol(100% combustion). If there is too much fuel for the air in the engine's cylinders then there will be a rich mixture. Combustion will not be complete and some fuel will remain unburn. This unburned fuel will exhaust into the atmosphere as gas and cause pollutions. If the mixture is very rich there will be a black smoke from the exhaust. If there is not enough fuel for the air in the cylinders, there will be a lean mixture. This could cause hard starting, poor combustion and loss of power (May, 2003).

Even though the ratio of air to fuel is correct in the engine's cylinder, not all the fuel will burn completely, it's depend on how well the air and fuel mix up in the cylinder. A better mixture will produce good combustion and engine efficiency. So, the air flow efficiency of the intake system is actually has a direct impact on the engine efficiency (May, 2003).

This study examines the flow in the air intake system and modified the air intake system to form a swirl air flow and minimize the pressure drop in the air intake system before enter the combustion chamber. All the analysis are carried out and proved using computational fluid dynamics (CFD) simulations.

### **1.3 PROJECT OBJECTIVES**

The objectives of this project are:

- i. Study the characteristics of the air flow motion in the existing model of Proton Waja 1.6L engine air intake system.
- ii. To compare the characteristics of the air flow motion in the new design air intake system with guide vane with the existing model of Proton Waja 1.6L engine air intake system (without guide vane).

### **1.4 SCOPES OF STUDY**

The scope of project covered study and analysis about characteristics of air flow in the Air Intake System (AIS) and analysis of the change in internal changes effect in the AIS. The scope of this project consists of this below:

- i. Analysis the pressure drop using engine speed from 1000r.p.m to 6000r.p.m.
- ii. Compare with developed guide vane air intake system with without developed guide vane air intake system through pressure losses percentage difference.
- iii. Analyze the effect of developed guide vane through velocity increment.

## **CHAPTER 2**

### **LITERATURE REVIEW**

#### **2.1 AIR INTAKE SYSTEM**

The work of an air filter is to filter the dirt particles from the intake air and supply cleaner air to the automobile engine. Air enters the filter through dirty pipe and inlet side plenum, which guides the flow uniformly through the filter media. Optimum utilization of filter can significantly reduce the cost of filter replacements frequently and keep the filter in use for longer time. To optimize intake system and filter, thorough understanding of flows and pressure drop through the system is essential.

An intake, or especially for car inlet is an air intake for an engine where the combustion engine is in essence a powerful air pump like the exhaust system on an engine, the intake must be carefully engineered and tuned to provide the greatest efficiency and power. Car engines need to breathe freely and easily for best performance, just like we do when we're exercising. Since car engines create power through combustion, getting enough air is vital. They won't work without it. The more air that gets into an engine, the better it will breathe. Also, engines give their best performance when the air they receive is cold. The cold air thickens the air/fuel mixture the engine burns, which allows the engine to get more energy out of it. An ideal intake system should increase the velocity of the air until it travels in to the combustion chamber, while minimizing turbulence and restriction of flow (May, 2003).

## 2.2 HELIX SHAPE

In mathematics, a helix is a curve in 3-dimensional space. The following parameterization in Cartesian coordinates defines a helix:

$$x(t) = \cos(t) \quad (2.1)$$

$$y(t) = \sin(t) \quad (2.2)$$

$$z(t) = t \quad (2.3)$$

As the parameter  $t$  increases, the point  $(x(t), y(t), z(t))$  traces a right-handed helix of pitch  $2\pi$  and radius 1 about the  $z$ -axis, in a right-handed coordinate system. In cylindrical coordinates  $(r, \theta, h)$ , the same helix is parameterized by:

$$r(t) = 1 \quad (2.4)$$

$$\theta(t) = t \quad (2.5)$$

$$h(t) = t \quad (2.6)$$

A circular helix of radius  $a$  and pitch  $2\pi b$  is described by the following parameterization:

$$x(t) = a \cos(t) \quad (2.7)$$

$$y(t) = a \sin(t) \quad (2.8)$$

$$z(t) = bt \quad (2.9)$$

Another way of mathematically constructing a helix is to plot a complex valued exponential function ( $e^{ix}$ ) taking imaginary arguments as shown in Eq. (2.10) (Euler's formula).

$$e^{ix} = \cos x + i \sin x \quad (2.10)$$

Except for rotations, translations, and changes of scale, all right-handed helices are equivalent to the helix defined above. The equivalent left-handed helix can be constructed in a number of ways, the simplest being to negate any one of the  $x$ ,  $y$  or  $z$  components (Bonner, J.T., 1951)

### **2.3 SWIRLS**

Swirling flows occurs in a very wide range of application both in nonreacting and reacting system. In nonreacting cases, applications include, for example cyclone separators, spraying systems, jet pumps, and many others. In combustion systems, it is applied in various systems such as gas turbines, utility boilers, industrial furnaces, internal combustion engines, and many other practical heating devices (N.A. Chigier, and A. Chervinsky, 1967). Swirling jets are used as means of controlling flames and the benefits of introduction of swirl in flame stabilizer design for industrial burners have been recognized. Swirling flows help to increase burning intensity through enhance mixing and higher residence time. It also helps in flame stabilization by the formation of secondary recirculating flows. Additionally, swirl that occurs in practical combustion system normally involves turbulent (T.H. Lin, and S.H. Sohrab, 1987) . Flame propagation in the turbulent flow fields involves complex flame flow interactions. One of the basic interactions of this type is that the rotating gas flow crossing the flame front. Knowing the importance of rotating flame as one of the basis to understand complex process of flame-flow interactions several investigations on rotating Bunsen burner has been performed (G.I. Sivashinski, and S.H. Sohrab, 1987)( G.I. Sivashinski, Z. Rakib, M. Matalon, and S.H. Sohrab, 1988). The influence of centrifugal and Coriolis accelerations on the shape, stability, and extinction limits of premixed flames was investigated (T. Kawamura, K. Asato, and T. Mazaki, 1980). Among other observations, it was found that flame stabilization by the burner rim is possible only at sufficiently low angular velocities. Under rapid rotation, the flame flashes back inside the burner tube (A.K. Gupta, D.G. Liley, and N. Syred, 1984). The basic influence of the burner rim hydrodynamics on stabilization of Bunsen flames has been emphasized in one study. In another theoretical investigation the effect of rotation on stabilization and geometry the effect of rotation on stabilization and geometry of Bunsen flames that are situated inside



rotating tubes was addressed. In the study, it was found that the rotation of the gas tends to reduce flame stabilization since flame flashback occurs at higher values of the mean flow velocity through the burner (J.M. Beer, N.A. Chigier, and K.B. Lee, 1963).

### 2.3.1 Low Swirl

Low swirl phenomena ( $S < 0.4$ ) typically are those for which the swirl velocity does not cause the flow structure to be drastically changed. As shown schematically in Figure 2.1, jet flow with this type of swirl often results in significant lateral pressure gradients only. Compared to its nonswirling counterpart, the jet produced by low degree of swirl is wider and slower. Flames with low degree of swirl have a limited practical interest mainly due to the instability problems. But similar to any other fundamental research this low swirl phenomenon is undeniably important for providing a useful ground in modeling purposes.

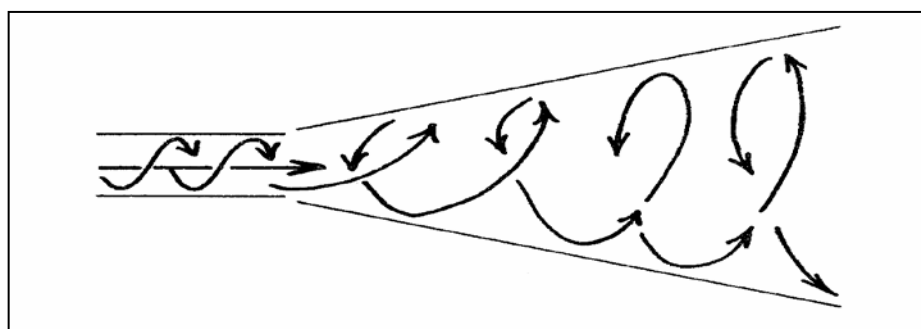


**Figure 2.1:** Jet flow with low degree of swirl ( $S < 0.4$ ) resulting in significant lateral pressure gradients only. Compared to its nonswirling counterpart, the jet produced is wider and slower.

Source: A.D. Birch, D.R. Brown, M.G. Dodson, and J.R. Thomas, 1987

But there are also cases where low swirl causes change in flow structure, meaning it may possess region of recirculation. Recirculation region in low swirl application are due to geometrical constraint such as shown in the flow around bluff-body flame holders, 'V' gutter-type flame stabilizers, quarl or divergent nozzle, and

sudden expansions of flow cross-sectional area. In this dissertation the emphasis has been given to low swirl and no axial recirculation zones. In some low swirl application, such as fire whirls, swirl is responsible for the lengthening of the flame, as discussed by Gupta et al (A.D. Birch, D.R. Brown, M.G. Dodson, and J.R. Thomas, 1987)

### 2.3.2 High Swirl

At high degree of swirl ( $S \geq 0.6$ ), radial and axial pressure gradients is large enough to cause an axial recirculation in the form of a central toroidal recirculation zone (CTRZ), which is not observed at lower degrees of swirl (Y.C. Chao, J.M. Han, and M.S. Jeng, 1990).

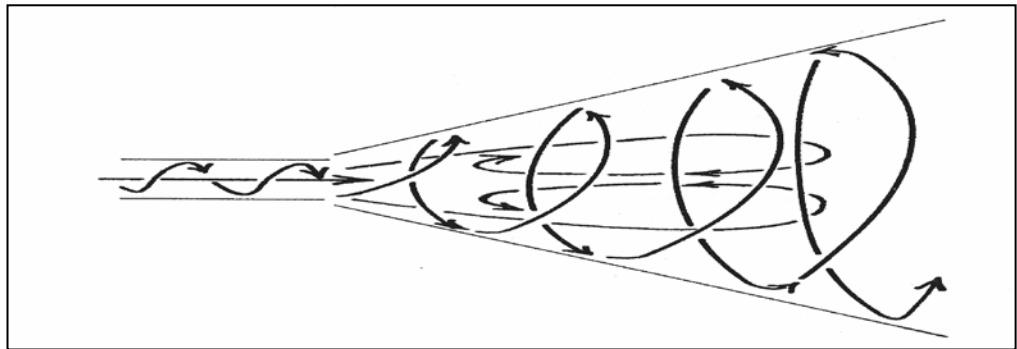


**Figure 2.2:** Jet flow of high degree of swirl ( $S > 0.6$ ) resulting in significant lateral as well as longitudinal pressure gradients. Compared to its nonswirling counterpart, the jet is much wider, slower and with a central toroidal recirculation zone.

Source: A.D. Birch, D.R. Brown, M.G. Dodson, and J.R. Thomas, 1987

Shown schematically in Figure 2.2, jet flow of high degree of swirl often results in significant lateral as well as longitudinal pressure gradients. Compared to its nonswirling counterpart, the jet is much wider, slower and with a central toroidal recirculation zone. In combustion, the presence of the recirculation zone plays important role in flame stabilization by providing a hot flow of recirculated combustion products and a reduced velocity region where flame speed and flow

velocity can be matched. Swirls also act to shorten the flame length and this is advantageous for having more compact burner design (Y.C. Chao, J.M. Han, and M.S. Jeng, 1990).

### **2.3.3 Generation of Swirl Flow**

Introducing rotation in the stream of fluid can be achieved by the following three principal methods: tangential entry of the fluid stream (axial-plus-tangential entry swirl generator), guided vanes (moving block or vane-type swirler) or simply by direct rotation (rotating tube) (A.D. Birch, D.R. Brown, M.G. Dodson, and J.R. Thomas, 1987).

### **2.3.4 Tangential Entry (Axial-Plus-Tangential Entry Swirl Generator)**

Figure 2.3 shows a (axial-plus-tangential entry) swirl generator that has been used for providing uniform stable jets for detailed experimental study. The quantities of air can be controlled and metered separately so that simply by adjusting the airflow rates the degree of swirl can be varied from that of zero swirl to that of a strongly swirling jet with reverse flow. Total pressure requirements of this system are relatively high, and commercial burners have tended to adopt the guided vane system, where vanes are so positioned that they deflect the flow direction (S C Kale and Prof V Ganesan, 2005)

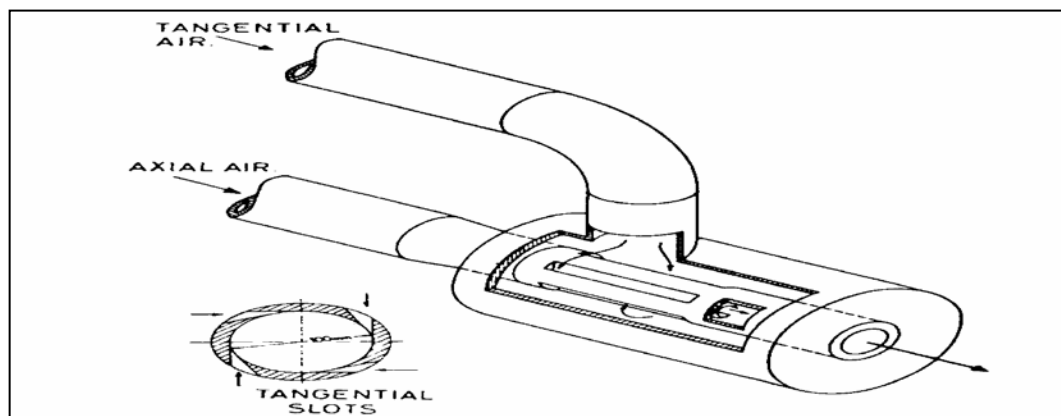


**Figure 2.3:** Swirl generator

Source: S C Kale and Prof V Ganesan, 2005

### 2.3.5 Guide Vanes (Moving Block Or Vane-Type Swirler)

In radial flow into a swirl generating device, radial and tangential vane angles can be altered in situ via the movable block swirl generator, which is really akin to the tangential entry method. The movable block system, shown in Figure 2.4, is efficient in that pressure drop required for producing a certain swirl level is relatively low, and high swirl strengths are obtainable.

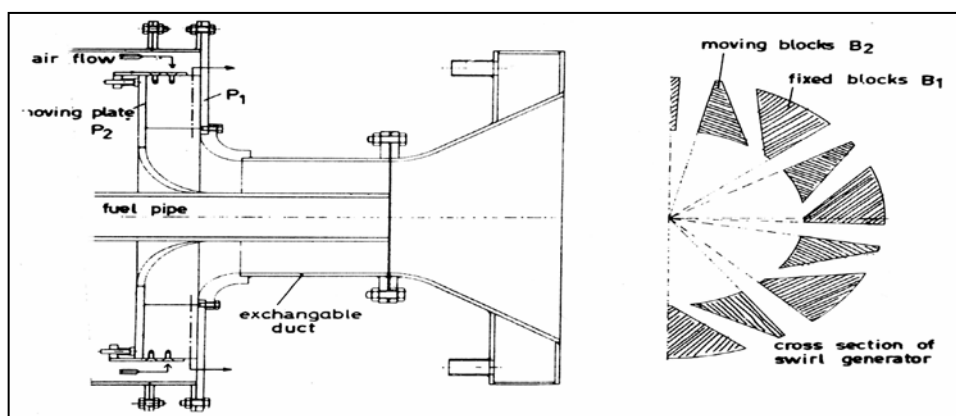


**Figure 2.4:** Moving block swirl burner.

Source: Pär Nylander, 2008

Figure 2.5 is an example of double concentric swirl burner developed by Gupta et al. The burner consists of a central nozzle surrounded by two concentric

annuli. Each annulus of the burner can be given desired swirl, either co- or counter-swirl by changing the direction of the swirler and the angle of the vane angle.

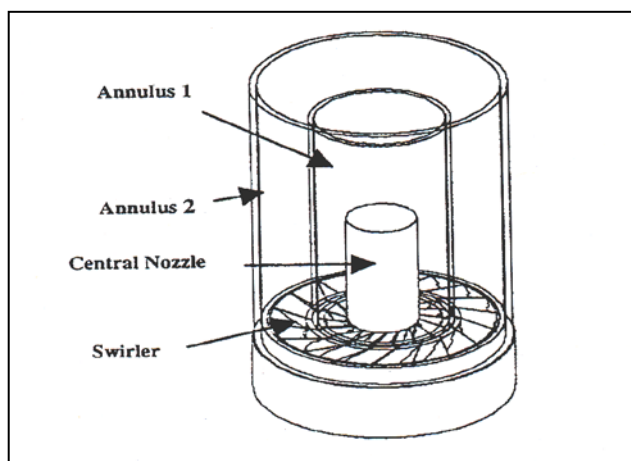


**Figure 2.5** Double concentric swirl burner

Source: Pär Nylander, 2008

In axial pipe flow, shown in Figure 2.6, a vane-type swirler consists of a fixed set of vanes at certain angle to the mainstream direction, which deflects the stream into rotation. This technique is common in furnaces and gas-turbine combustors. Generally, the vanes are mounted on a central hub and the vanes occupy the space in the annular region around it. Hubless swirler has been used in an attempt to improve outlet conditions, but separation and blade stall give complex flow patterns, and axisymmetry fails (A.D. Birch, D.R. Brown, M.G. Dodson, and J.R. Thomas, 1987)

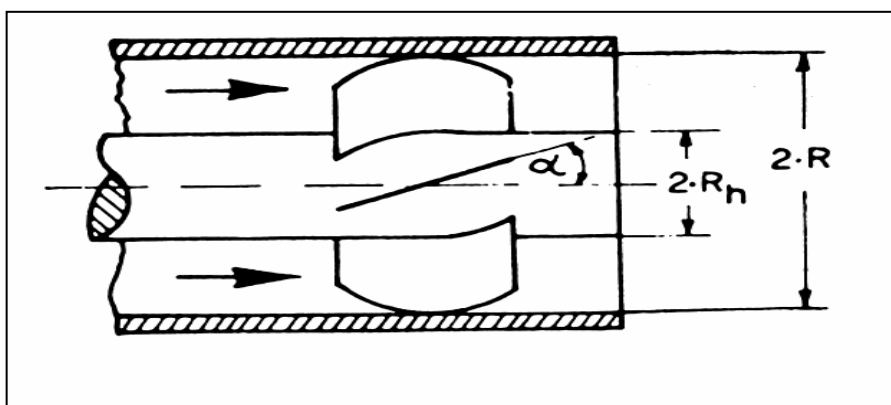


**Figure 2.6:** Vane-type swirler in an axial tube flow

### 2.3.6 Direct Rotation

Swirl may also be generated by direct rotation of the flow to induce a swirl motion solely by frictional drag of the cylinder wall upon the air stream passing through it. Since viscosity of air is small, the swirl effect is less seen in the fluid stream. That is why in some system, layers of honeycomb, or perforated plates or bundles of tubes are put in the middle of the rotating tubes. These kind of systems give exit velocity profiles of the 'solid body rotation' type in which the fluid particles are attached to the disk rotating with a constant angular velocity (May, 2003). The advantage of having rotating tube is that rotation is much easier to be controlled either at low or high rotational speed. The low burner rotational speed will also enable one to see the effect it will give on the flame stabilized at very low mixture velocity. Figure 2.7 shows an example of burner setup that producing rotating flame through tube directly rotated by dc motor .

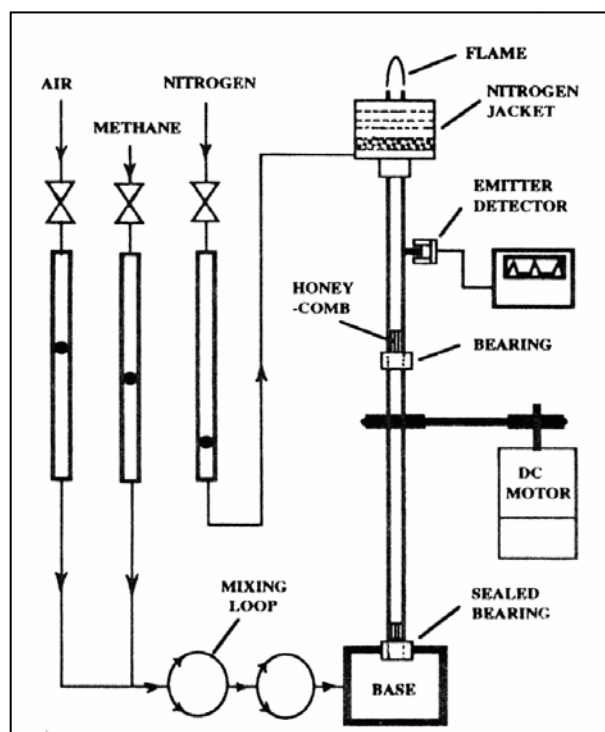


**Figure 2.7:** Rotating burner setup

In viscous fluid dynamics, rotating flows (that is, vortices) always possess a central core of solid body. Outside the central region, free (or potential) vortex conditions may prevail as are found in the atmosphere as whirlwinds, tornadoes,

hurricanes and cyclones. Fire whirls that occur in forest and urban fires may be simulated in the laboratory by rotating a large cylindrical wire screen. Figure 2.8 shows the experimental setup of rotating screen for fire whirl experiment.

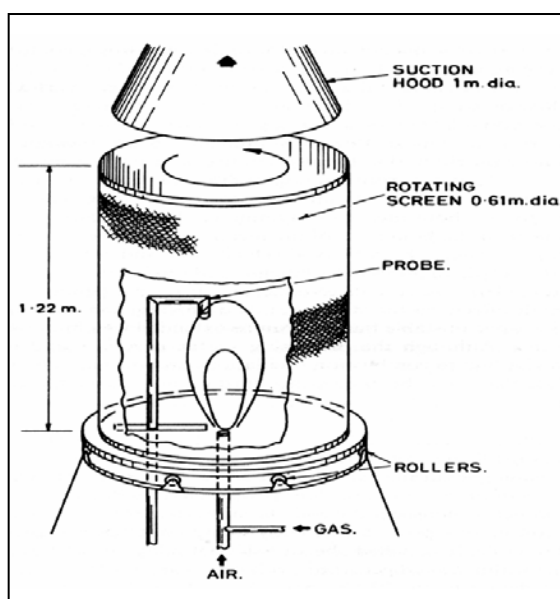


**Figure 2.8:** Rotating screen for fire whirl experiment and the example of the fire kindled in that type of experiment

Source: Y.C. Chao, J.M. Han, and M.S. Jeng, 1990

## 2.4 FLOW RATES IN HORIZONTAL PIPE

Air flow occurs only when there is a difference between pressures. Air will flow from a region of high pressure to one of low pressure. Figure 2.9 shows flow in the horizontal pipe. The change in pressure are given in Eq. (2.11). The volume flow rate are then given in the Eq. (2.13).

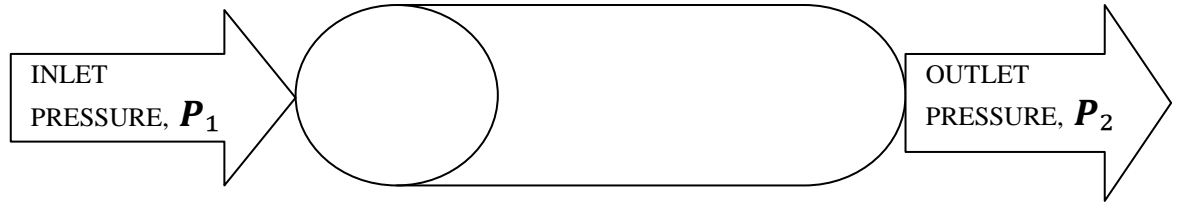


**Figure 2.9:** Flow in the horizontal pipe

$$\Delta P = P_1 - P_2 \quad (2.11)$$

$$Ac = \frac{\pi D^2}{4} \quad (2.12)$$

$$\tilde{V} = \frac{(\Delta P - \rho g L \sin \theta) \pi D^4}{128 \mu L} \quad (2.13)$$

**NOTE:** This equation only valid for laminar flow (S C Kale and Prof V Ganesan, 2005).

## 2.5 PRESSURE DROP AND HEAD LOSS IN A PIPE

In fluid mechanics the Reynold number is is a dimensionless number that the Reynolds number is proportional to inertia force/ viscous force and is used in momentum, heat and mass transfer to account for dynamic similarity. It can be defined in following form

$$Re = \frac{\rho V_{avg} D}{\mu} \quad (2.14)$$

If  $Re$  less than 2300, the flow is laminar and the friction factor,  $f$  and the head loss,  $h_L$  become

$$f = \frac{64}{Re} \quad (2.15)$$

$$h_L = \left( \frac{fL}{D2g} (V_{avg})^2 \right) \quad (2.16)$$

If  $Re$  more than 4000, the flow is turbulent and the friction factor,  $f$  and the head loss,  $h_L$  become



$$\frac{1}{\sqrt{f}} = -2.0 \log\left(\frac{\epsilon}{3.7} + \frac{2.51}{Re\sqrt{f}}\right) \quad (2.17)$$

$$\frac{1}{\sqrt{f}} = -2.0 \log\left(\frac{0.00042}{3.7} + \frac{2.51}{Re\sqrt{f}}\right) \quad (2.18)$$

While the different of change in pressure are as given in Eq. (2.19) and the head loss,  $h_L$  can be simplifies as in Eq. (2.21)

$$\Delta P = f \frac{L V^2}{D^2} \quad (2.19)$$

$$h_L = \left(\frac{fL}{D^2g} (V_{avg})^2\right) \quad (2.20)$$

$$h_L = \frac{\Delta P}{\rho g} \quad (2.21)$$

Note: The friction factor corresponding to this relative roughness and the Reynolds number van simply are determined from the Moody chart (refer to Appendix A). To avoid any reading error, we determine  $f$  from the Colebrook equation (S C Kale and Prof V Ganesan, 2005).

## 2.6 GOVERNING EQUATION

The equations governing the fluid are the continuity, momentum and turbulence model equations. According to the continuity equation, the rate of increase of fluid mass within a control volume is equal to the net rate of flow of mass into the control volume (Douglas, J.F, 1995).

## 2.7 REYNOLDS NUMBER EFFECT

The flow characteristics of wind passing across AIS pipe are depend on magnitude of inertial to viscous within the flow (the parameter are called Reynolds Number). The non-laminar flow in Reynolds number-from  $Re = 4 \times 10^3$  to  $Re = 10^8$ . The Reynolds Number is defined as for the flow that more than laminar flow the equation below used (S C Kale and Prof V Ganesan, 2005)

$$Re = v \frac{VD}{\nu} \quad (2.22)$$

Or

$$\text{Re} = \frac{\rho V L}{\mu} \quad (2.23)$$

Where  $V$  is the wind velocity,  $D$ ,  $L$  is the lateral dimension of the body,  $\nu$  is Kinematics viscosity of air,  $\mu$  dynamic viscosity of air and  $\rho$  is density of air.

This section contains a description of the characteristics of turbulence and the specification of turbulence model that used in fluent simulations. The equation is a ratio between the inertial and viscous forces in the fluid that determines the regime of the flow. When viscous forces dominates, the fluid travels smoothly in the domain and the forces acting for rapid fluctuations is suppressed by the forces acting to keep the flow in a steady behavior. The flow is then said to be laminar. On the other hand when the inertial forces dominate over the viscous forces and the Reynolds number is sufficiently large, the flow will become unsteady and fast fluctuations in the flow will occur. The flow is then said to be turbulent and a graphical description between laminar and turbulent flow is shown in the Figure 2.10.

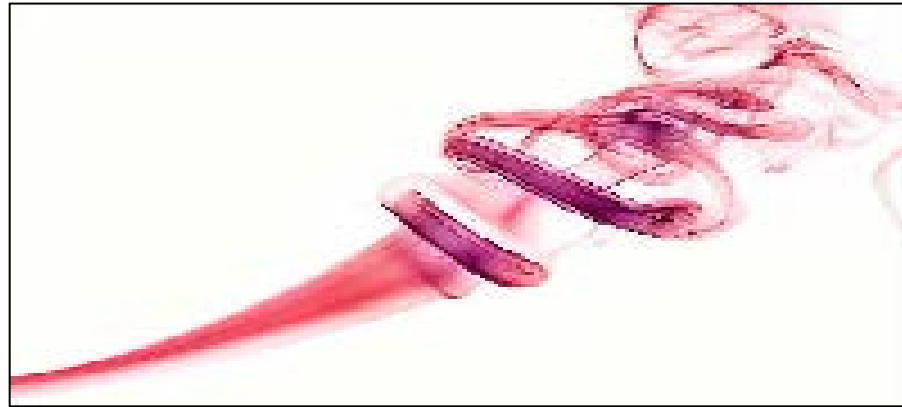


**Figure 2.10:** Transition between laminar and turbulent flow

Source: T.H. Lin, and S.H. Sohrab, 1987

The behavior of turbulent flows are more difficult predict than laminar flows since the presence of turbulence will make the flow unsteady (Pär Nylander, 2008).

### 2.7.1 Major Losses

The most pipe or duct system consists of the straight pipe at this point head loss due to viscous effect major losses can be determined by equation (S C Kale and Prof V Ganesan, 2005).

$$\text{Major losses, } h_{L \text{ major}} = f \frac{\ell}{D} \frac{V^2}{2g} \quad (2.24)$$

Friction factor,  $f$  to be determined using Moody chart. Using the Reynolds number and for the plastic surface of the AIS we look the graph curve at the graph smooth line. Because the roughness,  $\epsilon$ . For the turbulent developed flow, the value of  $f$  is simply (S C Kale and Prof V Ganesan, 2005).

$$\frac{1}{\sqrt{f}} \cong -1.8 \log \left[ \frac{6.9}{Re} + \left( \frac{\epsilon/D}{3.7} \right)^{1.11} \right] \quad (2.25)$$

### 2.7.2 Minor losses

In the intake system we found the system of the pipe more than a straight pipe. These additional components (valves, bends, tees, and the like) add the overall head loss of the system. Such losses are generally termed minor losses, with the corresponding head loss denoted Eq. (2.31) (S C Kale and Prof V Ganesan, 2005).

$$\text{Minor losses } h_{L \text{ minor}} = K_L \frac{V^2}{2g} \quad (2.26)$$

The most common method used to determine these head losses or pressure drops is to specify the loss coefficient,  $K_L$  Figure 2.11 which is defined as (Douglas, J.F, 1995).

$$K_L = h_{L \text{ minor}} \cdot \frac{2g}{V^2} = \frac{\Delta p}{\frac{1}{2}\rho V^2} \quad (2.27)$$

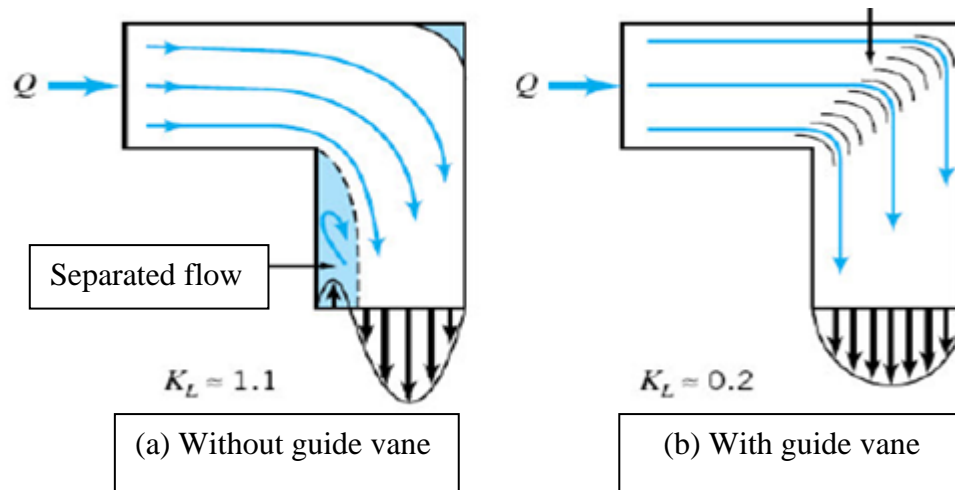


**Figure 2.11:** Difference between with and without guide vane

Source: Douglas, J.F,1995

$$\text{Pressure Drops, } \Delta p = K_L \frac{1}{2} \rho V^2 \quad (2.28)$$

## 2.8 Mass and Volume Flow Rate

The amount of mass flowing through a cross section per unit is called the mass flow rate and denoted by  $\dot{m}$ . The dot over a symbol is used to indicate time rate change (S C Kale and Prof V Ganesan, 2005).

$$\dot{m} = \rho V_{avg} A_c \quad (2.29)$$

We defined the average velocity  $V_{avg}$  average value across the entire cross section of the pipe, where  $A_c$  is the *area* of the cross section normal t the flow direction.

The volume of the fluid flowing through a cross section per unit time is called volume flow rate  $\dot{V}$  or  $Q$ .

$$\dot{V} = V_{avg} A_c = V A_c \quad (2.30)$$

The mass and volume flow rates are related by (Douglas, J.F, 1995).

$$\dot{m} = \rho \dot{V} \quad (2.31)$$

## 2.9 AIR FLOW RATE REQUIRED BY THE ENGINE

The air flow rate required  $V_a$  can be calculated from equation below for the particular engine speed if the engine displacement is known.

$$V_a = \frac{\eta_v N D_i}{2} (m^3/s) \quad (2.32)$$

Where,  $V_a$  is the required engine air flow rate,  $m^3/sec$ ,  $\eta_v$  is the engine volumetric efficiency (assumed 85% for normal specification engine),  $N$  is engine speed, rpm and  $D$  is engine displacement,  $m^3$

## CHAPTER 3

### METHODOLOGY

This section is to be able hold to the systematic study of methods that need to be set to achieve the objective of the project. It will ensure that the project is completed according to the schedule. This section also lists all the relevant method that needed during the project or experiment. The flow of this project will carried out as shown in Figure 3.1.

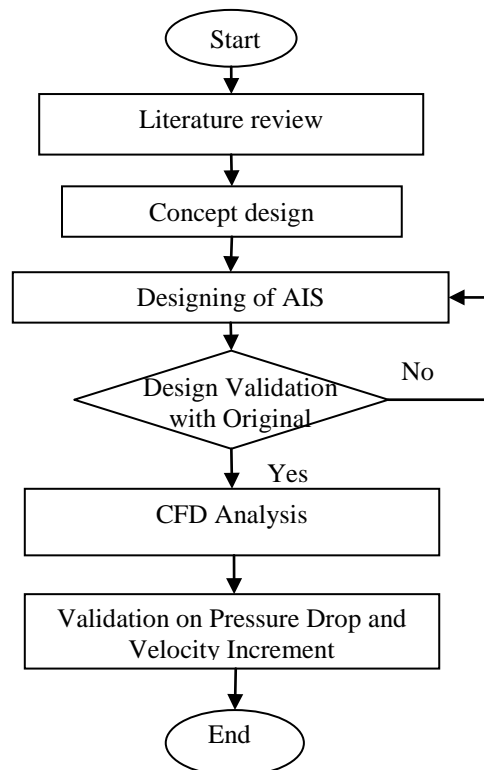


**Figure 3.1:** Methodology

### 3.1 GEOMETRY OF AIR INTAKE SYSTEM AND SIMPLIFICATION ON IT

The intake system that is used in this project is AIS of Proton Waja 1.6L engine. It is located just under the bonnet of the car close to the engine, as shown in Figure 3.2. The figure shows a photograph of the engine compartment taken from above.



**Figure 3.2:** AIS located under the bonnet

The system is divided into four section and numbered in Figure 3.2 which index denotes

1. Inlet dirt air duct (sucking area or path of air enters)
2. Intake section via pipe known as resonator
3. Filter box section (air cleaner)
4. Inlet to main intake manifold (throttle valve)

The inlet dirt air duct and intake section (resonator) is located right above the bonnet in the figure from which the air is guided into the filter box where the air is

cleaned. The air is then led through the filter, located inside the filter box but is not visible, to the inlet to the main engine as shown with the arrow pointing to the left.

### **3.2 MEASUREMENT AND MODELING**

The car model is Proton Waja 1.6L Engine (year 2000 model) and AIS were taken to Flow bench analysis lab. Besides collecting the car's overall dimension from its user manual, the AIS dimension was measured manually as it is not stated in the user manual. The manual measurement process was done using measuring tape, Vernier caliper, micrometer and some other measurement aiding tools. The measurements were double checked with taking 5 repeating reading to avoid significant errors.

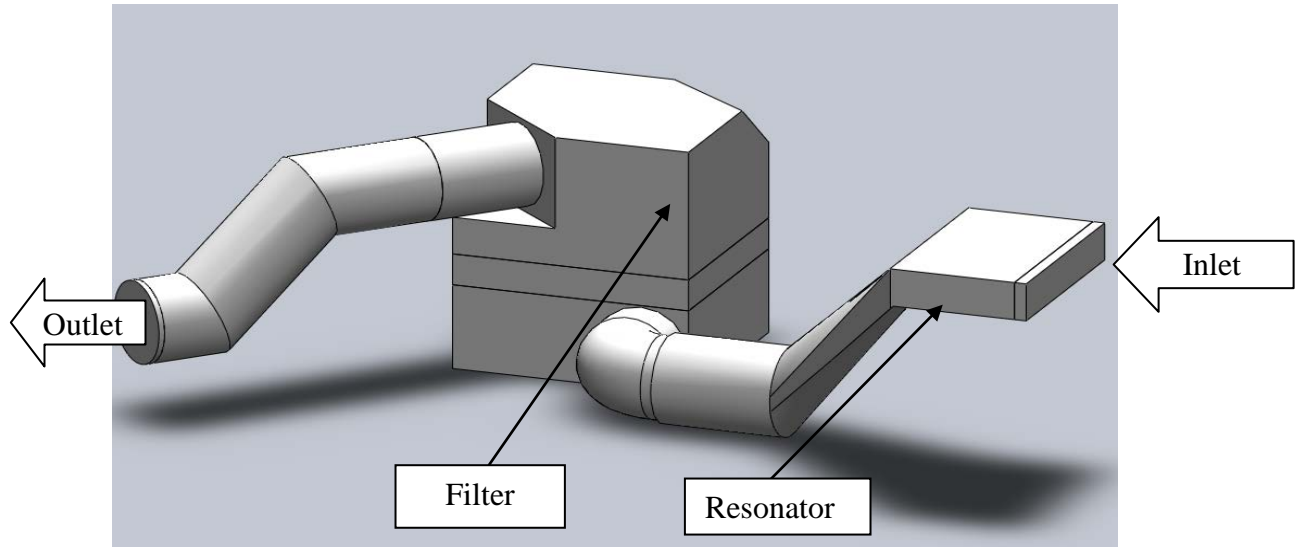
### **3.3 3-D MODELING SOFTWARE**

After measuring all the parts in AIS, the next step is to model it in 3-D software. The software that used to model this system is Solid Works 2009. By referring to the dimensions that was manually measured, it is transferred into a 3-D model Solid Works 2009. The Solid Works 2009 is also used to add swirl device in the AIS of the Proton Waja 1.6L (year 2000 model) in order to do the CFD analysis and simulation. The AIS dimension and rough sketch of the model were taken and the existing model was modeled in the Solid Works 2009. Total of six parts of the AIS were drawn separately before the AIS of the modeled were assembled to get the similar existing model features. The parts drawn separately requires correct dimension before it is assembled, if incorrect data were drawn the assembly may fail to run corresponding to the leakage or cannot fix the part correctly.



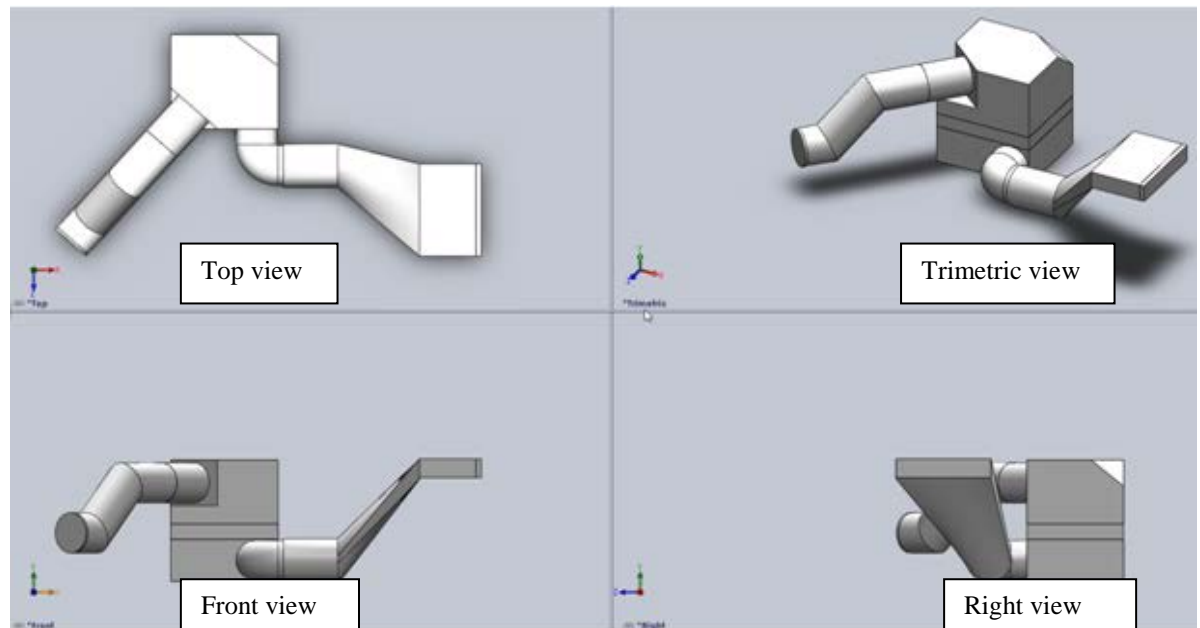
### 3.4 SOLID WORKS MODEL

Figure shows the AIS of Proton Waja 1.6L (year 2000 model) in Solid Works drawing.



**Figure 3.3:** AIS of Proton Waja 1.6L (year 2000 model)

A model of the air intake system is shown in Figure 3.3 above and there we can see how the air intake system is constructed in detail. Figure 3.4 below show AIS of Proton Waja 1.6L (year 2000 model) from different angles.



**Figure 3.4:** AIS of Proton Waja 1.6L (year 2000 model) from different angles

### 3.5 CFD CONDITION

#### 3.5.1 Computational Fluid Dynamics Simulation

Advanced computer simulation tools known as CFD (Computational Fluid Dynamics) have been employed in automotive development over the past few years. CFD simulations do not require real vehicles, CAD models are enough. These days extensive virtual simulations are performed on tens of computer processors even before the first prototypes are produced.

CFD codes provide numerous possibilities of making the air-flow along and inside vehicles visible in any views and with any degree of detail. Nonetheless, expert users explore much more than just air-flow along the body where other parts of vehicle taken into consideration too. For example, the heat extraction inside the

vehicle cabin to the environment. Many hours spent on guiding the air because the current vehicle cabins require efficient cooling and enough air to achieve maximum possible efficiency levels.

After Proton Waja 1.6L Engine AIS modeling is completed, the next process is to transfer the model into CFD Simulation known as Computational Fluid Dynamics Simulation to make analysis on the volume flow rate and the pressure distribution in the AIS.

This CFD simulation is to determine the difference in the AIS pressure drops and volume flow rate before and after the guide vane added. This CFD simulation does not need accurate dimensions as little change in measurement will not affect the result. By means, the AIS are considered as a closed boundary with two openings.

This simulation generally focuses on the pressure distribution in the AIS and the effect of flow of air in to the AIS after entering desired input of air flow rate with different setting of rpm. CFD simulation will show the most of the region that drops will occur and the different in the flow rate. During this simulation, all data were recorded and the analysis results were compared after all simulations done.

### 3.5.2 CFD Simulations Of The AIS

The process of designing the AIS continues to achieve the criteria set earlier in the concept stage. Simulation needs to be done to save time and cost of designing the AIS. As the air flow in the AIS is governed by fluid mechanics, the simulation of fluid motion would be needed to analyze the AIS. A computational method is chosen to calculate the fluid dynamics motion, by using a CFD package.

CFD generally solves fluid motion by solving the Navier-Stokes equation of mass, momentum and energy equation. The three equations can be written in the conservation form as follows:

$$\frac{\partial \rho}{\partial t} + \frac{\partial}{\partial x_k} (\rho u_k) = 0 \quad (3.1)$$

$$\frac{\partial \rho u_i}{\partial y} + \frac{\partial}{\partial x_k} (\rho u_i u_k - \tau_{ik}) + \frac{\partial P}{\partial x_i} = S_i \quad (3.2)$$

$$\frac{\partial(\rho E)}{\partial y} + \frac{\partial}{\partial x_k} ((\rho E + P)u_k + q_k - \tau_{ik}u_i) = S_k u_k + Q_H \quad (3.3)$$

where  $u$  is the fluid velocity,  $\rho$  is the fluid density,  $S_i$  is a mass-distributed external force per unit mass,  $E$  is the total energy per unit mass,  $Q_H$  is a heat source per unit volume,  $\tau_{ik}$  is the viscous shear stress tensor and  $q_i$  is the diffusive heat flux.

Turbulence normally occurs in any fluid flow. To predict turbulent flow, the Reynolds averaged Navier-Stokes equations will be used. Through this procedure, extra terms known as the Reynolds stresses would appear in the equations. Following Boussinesq's assumption, the Reynolds stresses would then be defined in this model as:

$$\tau_{ij}^R = \mu_t \left( \frac{\partial u_i}{\partial x_j} + \frac{\partial u_j}{\partial x_i} - \frac{2}{3} \frac{\partial u_l}{\partial x_l} \delta_{ij} \right) - \frac{2}{3} \rho k \delta_{ij} \quad (3.4)$$

$\mu_t$  is defined using two basic turbulence properties, namely the turbulent kinetic energy,  $k$  and the turbulent dissipation,  $\varepsilon$ ,

$$\mu_t = f_\mu \frac{C_\mu \rho k^2}{\varepsilon} \quad (3.5)$$

Thus, the  $k - \varepsilon$  model is used to solve turbulence by the software package. Generally, the CFD analysis follows steps shown in Figure 3.1.

### 3.6 AIR PROPERTIES

The first boundary would be the air properties. The properties of air are taken as shown in Table 3.1. The values of pressure and temperature should be taken from an aneroid barometer from the lab. The other values are interpolated from fluid

dynamic air properties found in any fluid properties table at the given pressure and temperature. The air property would be used as the first input to the inlet of the AIS.

**Table 3.1:** Properties of air

<b>Properties</b>	<b>Value</b>
Pressure	101325 Pa
Temperature	300 K
Secific Heat, Cv	1006 J/kgK
Density, $\rho$	1.225kg/m <sup>3</sup>
Dynamic Viscosity, $\mu$	1.80x10 <sup>-5</sup> kg/ms

### 3.7 SPECIFICATIONS OF PROTON WAJA 1.6L

Table 3.2 shows the specification of proton Waja 1.6L (year 2000 model).

**Table 3.2:** Specification of proton Waja 1.6L

<b>Perfomance</b>	<b>Value</b>
Engine	4G18 S4 MPI with emission standard EC 94/12
Maximum Power	76kW @ 6000 rpm
Maximum Torque	140 Nm @2750 rpm
Bore and stroke	76.0 mm x 87.3 mm
Displacement	1584 cc
Maximum Speed	186 km/h
Filter Porosity	85%
Type of Fuel	Petrol

### 3.8 CALCULATION AND EQUATIONS

#### 3.8.1 Required Engine Air Flow Rate

The air flow rate,  $V_a$  required by the engine for the particular engine speed where the engine displacement is known.

$$V_a = \frac{\eta_v N D_i}{2} (m^3/s) \quad (3.6)$$

Where,

- $V_a$  The required engine air flow rate,  $m^3/sec$
- $\eta_v$  The engine volumetric efficiency (assumed 85% for normal Specification engine)
- $N$  engine speed, rpm
- $D_i$  engine displacement,  $m^3$

#### 3.8.2 Pressure Drop

Pressure drop across the AIS are calculated by referring to Figure 3.5.

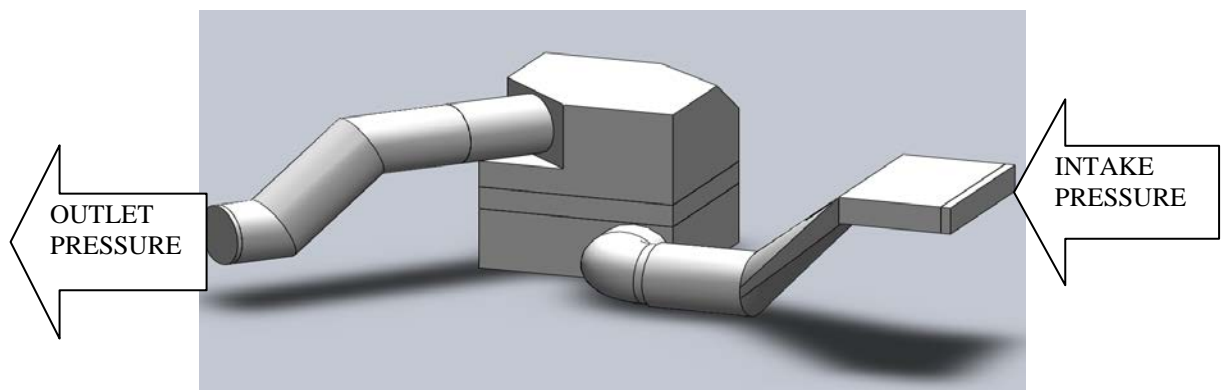


**Figure 3.5:** AIS of Proton Waja 1.6L (year 2000 model)

By considering  $P_1 < P_2$ , the pressure drop can be shown by the Eq. (3.7)

$$\Delta P = P_1 - P_2 \quad (3.7)$$

Where,

$\Delta P$  = change in pressure/pressure drop

$P_1$  = intake pressure

$P_2$  = outlet pressure

### 3.8.3 Pressure Drop Improvement

Percentage of pressure drop improvement can be calculated as:

$$\% \Delta P = \frac{\Delta P_1 - \Delta P_2}{\Delta P_1} \times 100\% \quad (3.8)$$

Where,

$\% \Delta P$  = percentage of pressure drop

$\Delta P_1$  = pressure drop across AIS without guide vane

$\Delta P_2$  = pressure drop across AIS with guide vane

## **CHAPTER 4**

### **RESULTS AND DISCUSSIONS**

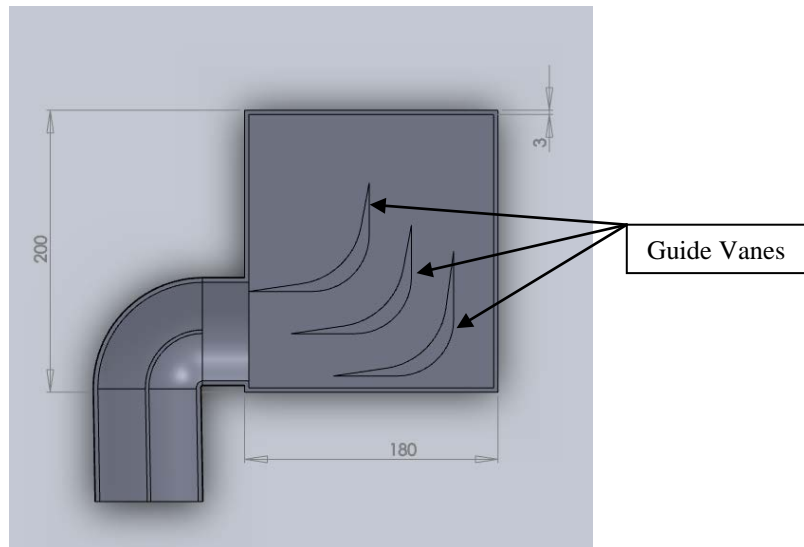
#### **4.1 INTRODUCTION**

Actual and modified AIS were drawn by using SOLIDWORK software. A CFD investigation or flow simulation was carried out under steady flow conditions and the air flow behavior in the AIS in such a way that the geometrical design was modified to increase the capabilities of the intake air enter the engine at high pressure and velocity. The modified AIS's result was validated against the actual AIS's result.

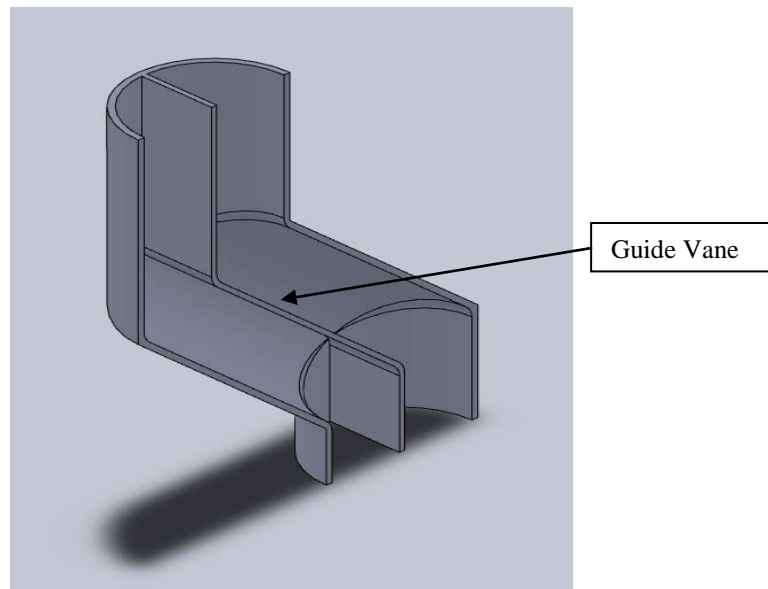
The inlet boundary condition was set at environmental pressure while the outlet boundary was set at air flow rate which required by the engine. The environmental pressure was set at 101325 Pa and the temperature at 300K. Heat transfer are not selected since this paper only studies on pressure drop in through the AIS and heat transfer are assumed to be negligible. So the walls of the AIS system are set to be adiabatic.

Figure 4.1 the down box and Figure 4.2 the outlet pipe shows the place where the guide vanes are placed in the modified CFD model. By adding this guide vane it will decreases the pressure drop which will keeps the pressure inside the AIS almost same to the atmospheric pressure. By minimize the pressure drop, the combustion in the combustion chamber will be more efficient.





**Figure 4.1:** Guide Vane placement on the down box.



**Figure 4.2:** Guide Vane placement on the outlet pipe.

## 4.2 PRESSURE DROP AND VELOCITY DIFFERENCE TABLE FOR WITHOUT GUIDE VANE AIS

Table 4.1 shows the pressure drop through the actual AIS (without guide vane) at different engine speed. It is found that the pressure drop is increased as the engine speed is increased. For example at engine speed 1000 rpm, the pressure drop is 18 Pa and it's increased to 71 Pa when the engine speed is 2000 rpm. This losses experienced by AIS will affect the AIS efficiencies during the combustion process.

**Table 4.1:** Pressure Drop for without guide vane

<b>Engine Speed (rpm)</b>	<b>Intake Pressure(Pa)</b>	<b>Outlet Pressure(Pa)</b>	<b>Pressure Drop(Pa)</b>
1000	101321	101303	18
2000	101306	101235	71
3000	101283	101122	161
4000	101250	100964	286
5000	101208	100770	438
6000	101157	100530	627

Table 4.2 shows the velocity improvement through the actual AIS (without guide vane) at different engine speed. It is found that the velocity improvement is increased as the engine speed is increased. For example at engine speed 1000 rpm, the velocity improvement is 0.18359 m/s and it's increased to 0.34647 m/s when the engine speed is 2000 rpm.

**Table 4.2:** Velocity Improvement for without guide vane

<b>Engine Speed (rpm)</b>	<b>Intake Speed (m/s)</b>	<b>Outlet Velocity(m/s)</b>	<b>Velocity Increment (m/s)</b>
1000	2.83533	3.01892	0.18359
2000	5.66666	6.01313	0.34647
3000	8.49311	9.18455	0.69144
4000	11.30960	12.3221	1.01250
5000	14.11510	15.4464	1.33130
6000	16.90740	18.5014	1.59400

### 4.3 PRESSURE DROP AND VELOCITY DIFFERENCE ANALYSIS FOR WITH GUIDE VANE AIS

Table 4.3 shows the pressure drop through the modified AIS (with guide vane) at different engine speed. It is found that the pressure drop is increased but not as much compare with the actual AIS as the engine speed is increased. For example at engine speed 6000 rpm, the pressure drop in actual AIS is 627 Pa but in modified AIS is only 501 Pa. This will increase the capabilities of the intake air enter the engine at high pressure and velocity.

**Table 4.3:** Pressure Drop for with guide vane

<b>Engine Speed (rpm)</b>	<b>Intake Pressure(Pa)</b>	<b>Outlet Pressure(Pa)</b>	<b>Pressure Drop(Pa)</b>
1000	101320	101303	17
2000	101304	101241	63
3000	101278	101145	133
4000	101242	101022	220
5000	101195	100844	351
6000	101138	100637	501

Table 4.4 shows the velocity improvement through the modified AIS (with guide vane) at different engine speed. It is found that the velocity improvement is increased as the engine speed is increased. For example at engine speed 1000 rpm, the velocity improvement is 0.04401 m/s and it's increased to 0.05739 m/s when the engine speed is 2000 rpm.

**Table 4.4:** Velocity Increment for with guide vane

<b>Engine Speed (rpm)</b>	<b>Intake Speed (m/s)</b>	<b>Outlet Velocity(m/s)</b>	<b>Velocity Improvement(m/s)</b>
1000	2.98442	3.02843	0.04401
2000	5.93612	5.99351	0.05739
3000	8.94101	9.03906	0.09805
4000	11.9125	12.0607	0.14820
5000	14.8728	15.0872	0.21440
6000	17.8213	18.11011	0.28881

#### **4.4 GRAPHICAL ANALYSIS DATA RESULT**

From the Figure 4.3 it is found that the pressure drop is directly proportional to the engine speed for both actual and modified AIS. When the engine is run at 1000 r.p.m (idle condition) the pressure drop for both actual and also for modified AIS are almost same and it is increase up to 627 Pa as the engine speed increased. This is because the pressure drop along the intake system is very dependent on engine speed and the cross sectional area of the AIS. Pressure drop in AIS without guide vane is much higher compare to pressure drop in AIS with guide vane. This can be seen from the graph in Figure 4.3. This is due to the guide vane which helps to minimize the pressure drop along the system especially at high engine speed. Refer APENDIX B to view clearly and compare the pressure distribution in the AIS for both actual and modified AIS.

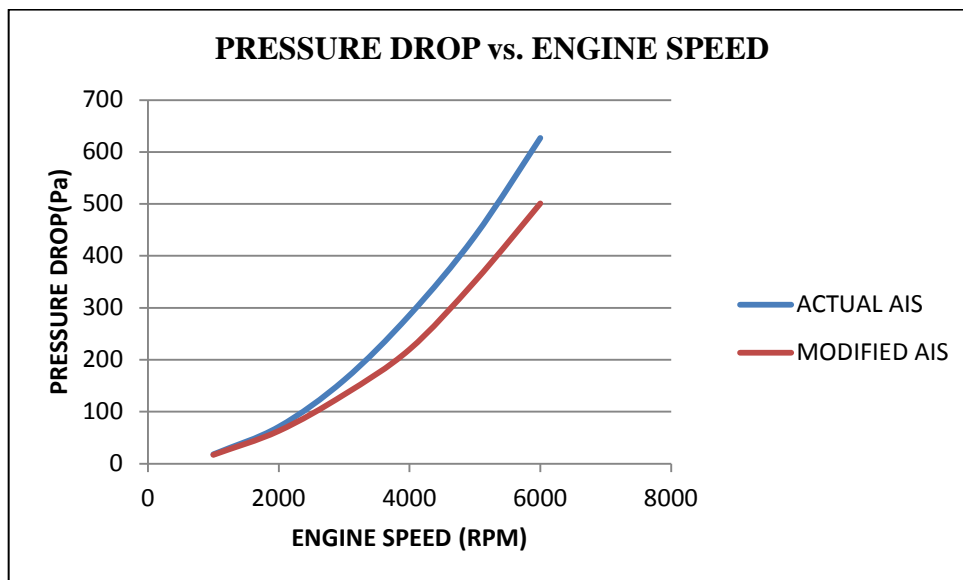


**Figure 4.3:** Graph of pressure drop vs. engine speed

From the Figure 4.4 it is found that the velocity improvement is directly proportional to the engine speed. It is also found that the velocity improvement for actual AIS is much greater compare with the modified AIS, but overall inlet and outlet velocity for modified AIS is much greater compare with actual AIS. It is shown in Figure 4.5 and Figure 4.6.

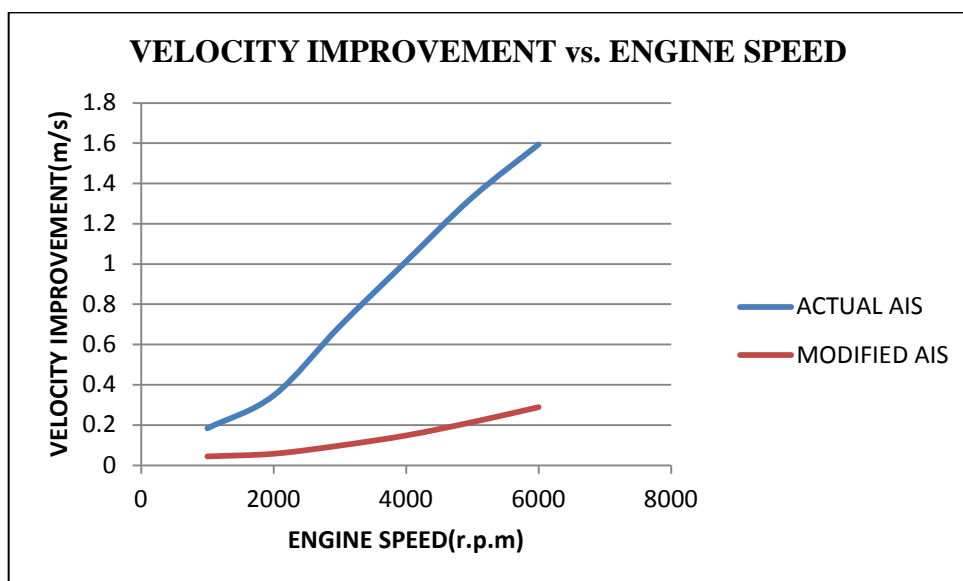


**Figure 4.4:** Graph of velocity improvement vs. engine speed

The inlet air velocity was improved and higher compare with the actual AIS because the guide vane which placed in the AIS creates a low pressure area which pull the air inside the AIS a high velocity. Beside that the outlet velocity for modified AIS is also higher compare with actual AIS because of high inlet velocity and low pressure drop. Refer APENDIX C to view clearly and compare the velocity distribution in the AIS for both actual and modified AIS.

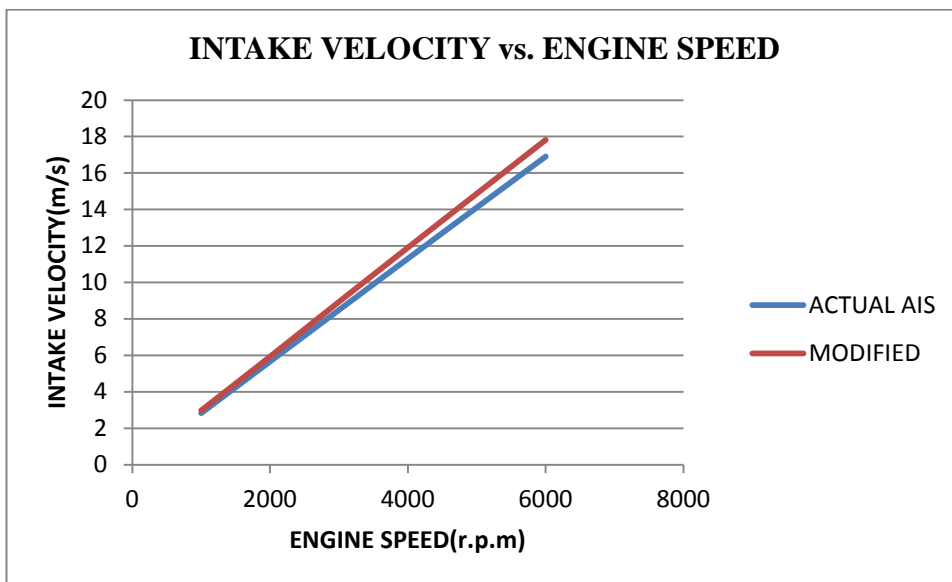


**Figure 4.5:** Graph of intake velocity vs. engine speed

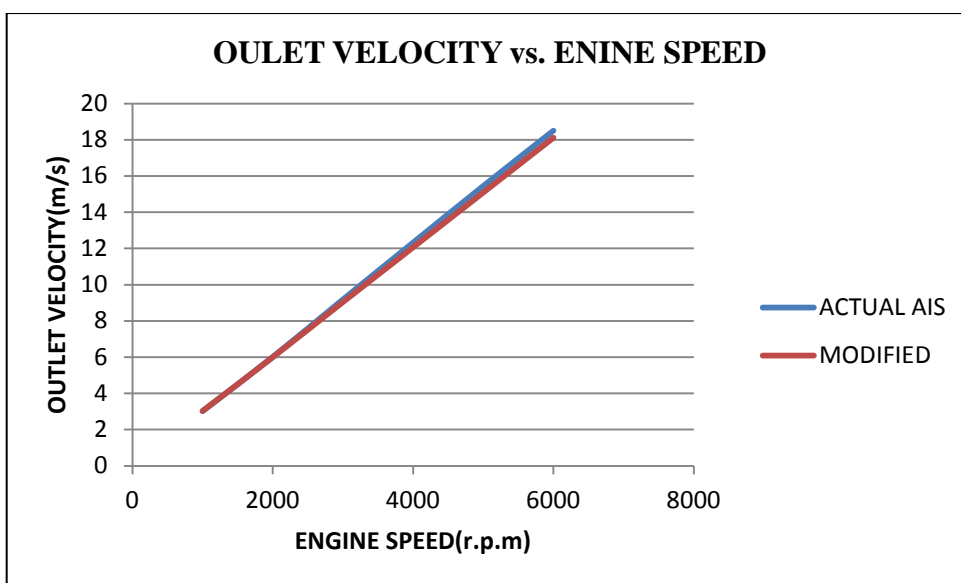


**Figure 4.6:** Graph of outlet velocity vs. engine speed

#### 4.5 RESULTS AND CALCULATION

The air volume flow rate required  $V_a$  can be calculated from Eq. 3.6 for the particular engine speed if the engine displacement is known. Example of air volume flow rate calculation for engine speed at 1000 r.p.m :

$$\begin{aligned} V_a &= \frac{\eta_v N D_i}{2} (m^3/s) \\ &= \frac{0.85 * 1000 * 1584 * 10^{-6}}{2(60)} (m^3/s) \\ &= 0.01122 m^3/s \end{aligned}$$

Table 4.5 shows the air volume flow rate that required by the engine at different engine speed. The engine volumetric efficiency and the engine speed are always constant that is 0.85 and 1584 cm<sup>3</sup> respectively. Air volume flow rate that required by the engine are directly proportional to the engine speed. At high engine speed the engine need more air for the combustion in the combustion chamber and at the same time the engine piston will move faster as the engine speed increase. The fast movement of the engine piston will suck the air from the AIS at high rate.

**Table 4.5:** Engine air flow rate calculation

<b>Engine Speed(r.p.m)</b>	<b>Engine Volumetric Efficiency (<math>\eta_V</math>)</b>	<b>Engine Displacement, <math>\text{cm}^3</math> (<math>D_i</math>)</b>	<b>Engine Air Volume Flow rate, <math>\text{m}^3/\text{sec}</math> (<math>V_a</math>)</b>
1000	0.85	1584	0.01122
2000	0.85	1584	0.02244
3000	0.85	1584	0.03366
4000	0.85	1584	0.04488
5000	0.85	1584	0.0561
6000	0.85	1584	0.06732

Table 4.6 shows the pressure drop across AIS for with and without guide vane placement. From the Table 4.6 for AIS without guide vane the pressure drop is only 18 Pa a engine speed 1000 r.p.m and its increased to 71 at engine speed 2000 r.p.m. while for engine speed 3000 r.p.m to 6000 r.p.m, the pressure drop is 161 Pa, 286 Pa, 438 Pa and 627 Pa respectively. While for AIS with guide vane the pressure drop at engine speed 1000 r.p.m to 6000 r.p.m is 17 Pa, 63 Pa, 133 Pa, 351 Pa and 501 Pa respectively. From this result we can conclude that the pressure drop is directly proportional to the engine speed. The pressure drop in AIS without guide vane is much higher compare with the pressure drop in AIS with guide vane.



**Table 4.6:** Pressure drop across AIS for with and without guide vane

	Pressure of air for AIS Without Guide Vane (Pa)		Pressure drop across the AIS (Pa)	Pressure of air for AIS With guide vane (Pa)		Pressure drop across the AIS (Pa)
	Intake	Outlet		Intake	Outlet	
Engine speed (r.p.m)						
1000	101321	101303	18	101320	101303	17
2000	101306	101235	71	101304	101241	63
3000	101283	101122	161	101278	101145	133
4000	101250	100964	286	101242	101022	220
5000	101208	100770	438	101195	100844	351
6000	101157	100530	627	101138	100637	501

Pressure Drop Improvement can be calculated using Eq. 3.8. Example of pressure drop improvement calculation for the engine speed at 1000 r.p.m:

$$\Delta P_i = \frac{\Delta P_1 - \Delta P_2}{\Delta P_1} = \frac{18 - 17}{18} = 0.055556 \text{ Pa}$$

Table 4.7 shows the percentage improvement in total pressure drop. The percentage of pressure drop improvement a engine speed 1000 r.p.m is 5.55556% and 11.2676% at engine speed 2000 r.p.m. while for engine speed 3000 r.p.m to 6000 r.p.m is 17.3913%, 23.0769%, 19.8630% and 20.0957% respectively. Total percentage of pressure drop improvement is 97.2501%. From this result we can conclude that by adding guide vane in the AIS is actually reduce the pressure drop in the system.

**Table 4.7:** Percentage improvement in total pressure drop

<b>RPM speed</b>	<b>Pressure drop improvement, <math>\Delta P_i</math></b>	<b>Percentage of pressure drop improvement, <math>\Delta P_i\%</math></b>
1000	0.055556	5.55556
2000	0.112676	11.2676
3000	0.173913	17.3913
4000	0.230769	23.0769
5000	0.198630	19.8630
6000	0.200957	20.0957
	$\Sigma\Delta P_i\%$	97.2501

Average percentage pressure drop improvements are

$$\Delta P_{ave} = \frac{\Sigma\Delta P_i}{7} \% = \frac{97.2501}{7} \% = 16.20835\%$$

So the average percentage pressure drop improvement is 16.20835%.

## **CHAPTER 5**

### **CONCLUSION AND RECOMMENDATION**

#### **5.1 CONCLUSION**

Actual and modified AIS were drawn by using SOLIDWORK software. A CFD investigation or flow simulation was carried out under steady flow conditions and the air flow behavior in the AIS in such a way that the geometrical design was modified to increase the capabilities of the intake air enter the engine at high pressure and velocity. The modified AIS's result was validated against the actual AIS's result.

From the analysis it can be concluded that the pressure drop and the air flow velocity is directly proportional to the engine speed. By adding the guide vane it decreases the pressure drop which keeps the pressure inside the AIS almost same to the atmospheric pressure. By minimize the pressure drop, the combustion in the combustion chamber might more efficient.

The objective of this project was achieved where the analyzed data shows positive result that is the pressure drop across the AIS was reduced by 16.20835% by adding guide vane in the AIS.

## 5.2 RECOMMENDATION

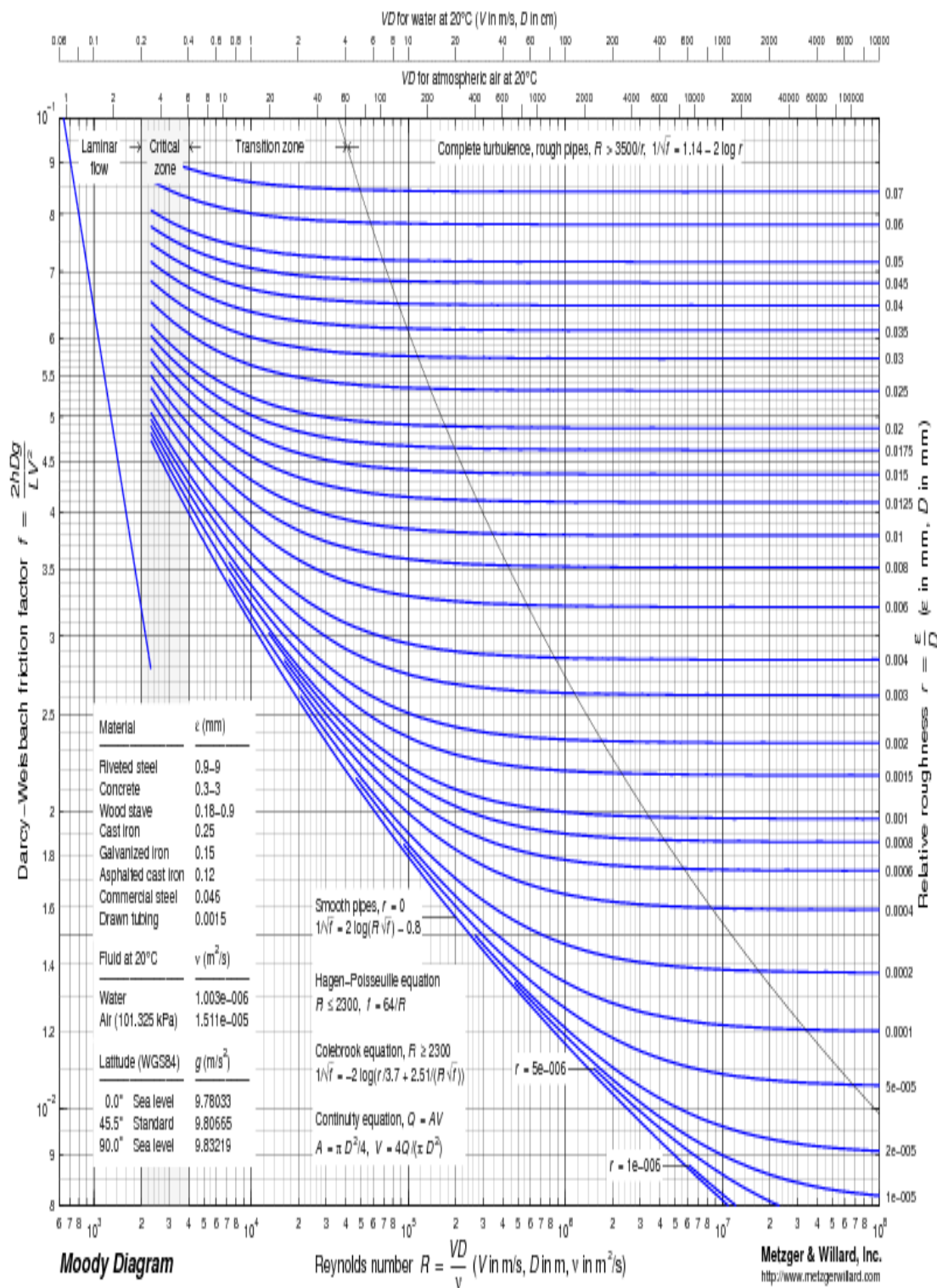
Some other recommendations:

- Design more guide vane placement and improve the design of AIS.
- Analyze the effect of noise in the AIS.
- Analysis effect of minimizing the length of AIS.
- Building duct that has more flow features that can guide the air.  
Introduction of bell-mouth in dirty and clean pipe.

## REFERENCES

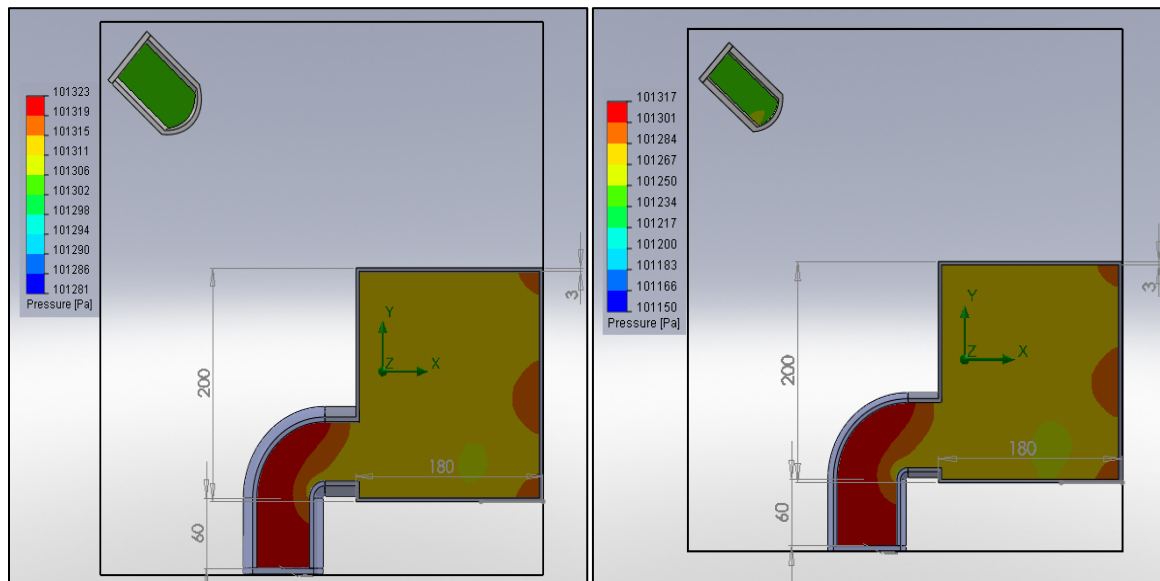
- A.D. Birch, D.R. Brown, M.G. Dodson, and J.R. Thomas (1978). The turbulent concentration field of a methane jet, *J. Fluid Mech.* 88 Part 3, pp.431.
- A.K. Gupta, D.G. Liley, and N. Syred. *Swirl Flows*, Abacus Press, Ohio, 1984.
- Bonner, J. T. (Mar. 1951). "The Horn of the Unicorn." *Sci. Amer.* 184, pp. 42-43.
- Douglas, J.F (1995) *Fluid Mechanics*, Longman Scientific & Technical, London.
- G.I. Sivashinski, and S.H. Sohrab (1987). *Combust. Sci. Technol.*, 53:67-74.
- G.I. Sivashinski, Z. Rakib, M. Matalon, and S.H. Sohrab (1988). *Combust. Sci. Technol.*, 57:37-53.
- J.D. Anderson (2009). *Computational Fluid Dynamics*.
- J.M. Beer, N.A. Chigier, and K.B. Lee (1963). Ninth Symposium (International) on Combustion, The Combustion Institute, Pittsburgh, pp. 892-900.
- May (2003). *Automotive Mechanics*. Mc Graw Hill, pp.180-198.
- N.A. Chigier, and A. Chervinsky (1967). Eleventh Symposium (International) on Combustion. The Combustion Institute, Pittsburgh, pp. 489-499.
- Pär Nylander. (2008). *CFD Modeling of Water Ingestion in Air Intake System*. Lulea University of Technology.
- P. A. Rusch and A. K. Dhingra. (2002). Numerical and Experimental Investigation of the Acoustic and Flow Performance of Intake Systems. *Journal of Vibration and Acoustics*.
- S C Kale and Prof V Ganesan. (2005). A Study of Steady Flow through a SI Engine Intake System using CFD. Department of Mechanical Engineering, Indian Institute of Technology, Madras, Chennai, India
- T.H. Lin, and S.H. Sohrab (1987). *Combust. Sci. Technol.*, 52:73-79.
- T. Kawamura, K. Asato, and T. Mazaki (1980). *Combust. Sci. Technol.*, 22:211-216.
- Y.C. Chao, J.M. Han, and M.S. Jeng (1990). A quantitative laser sheet image processing method for the study of the coherent structure of a circular jet flow, *Experiments in Fluids* 9, 323-332.
- W.W. Pulkrabek (1993). *Engineering Fundamentals of the Internal Combustion Engine*

APPENDIX A



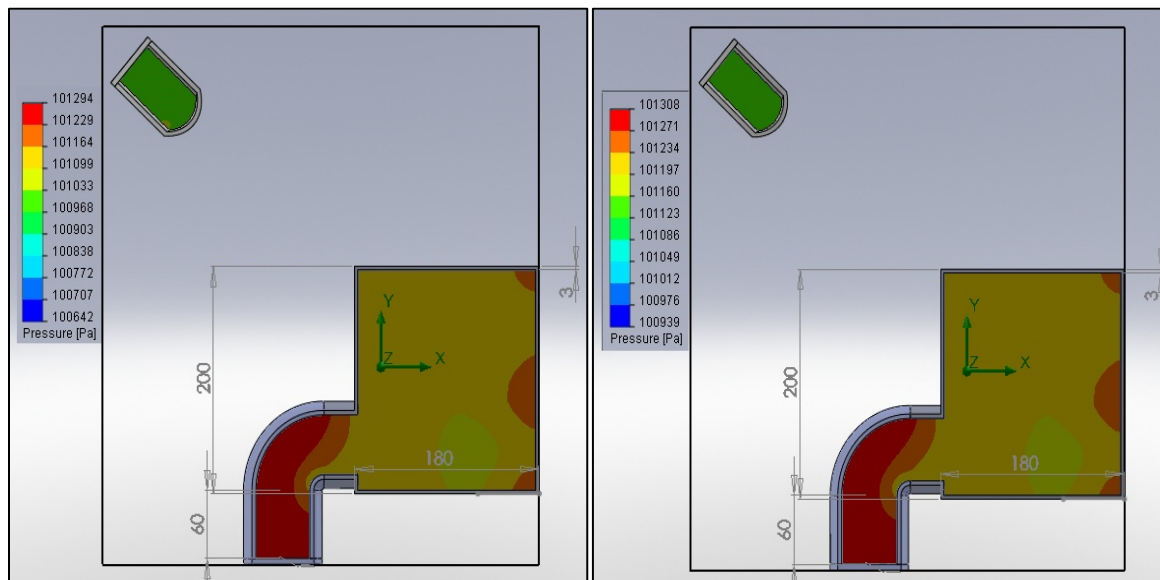
## APPENDIX B

## PRESSURE DISTRIBUTION (WITHOUT GUIDE VANE) AT VARIOUS ENGINE SPEED



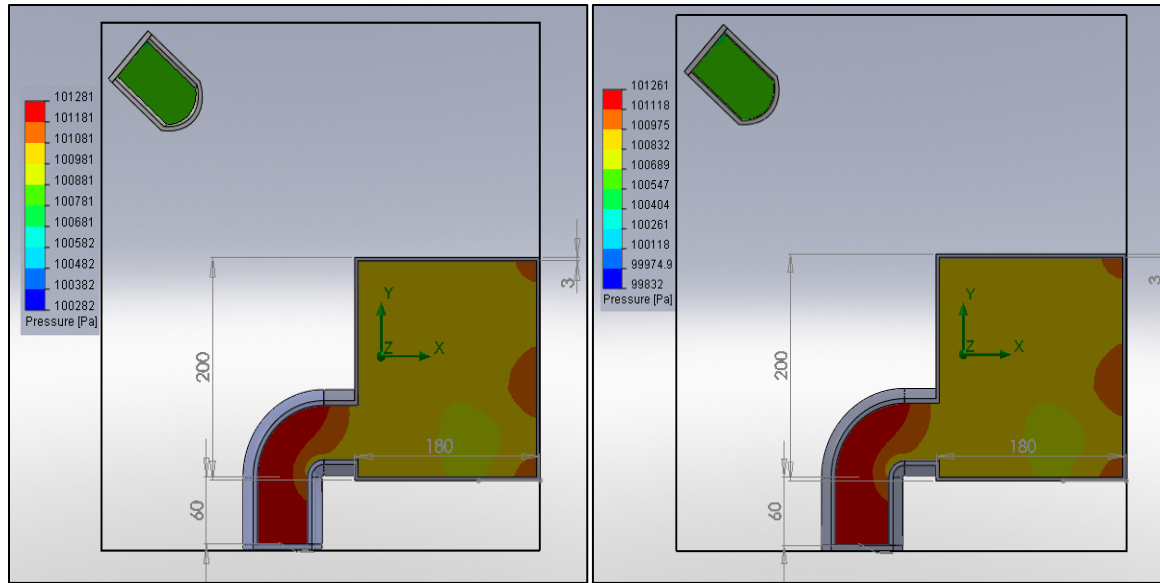
1000 r.p.m

2000 r.p.m



3000 r.p.m

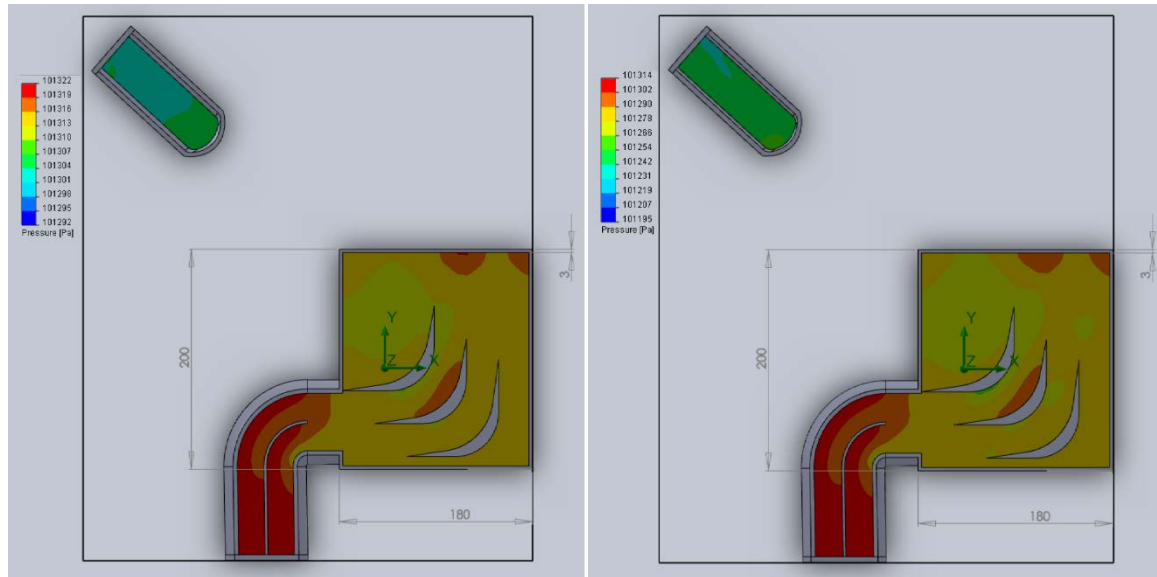
4000 r.p.m





## APPENDIX C

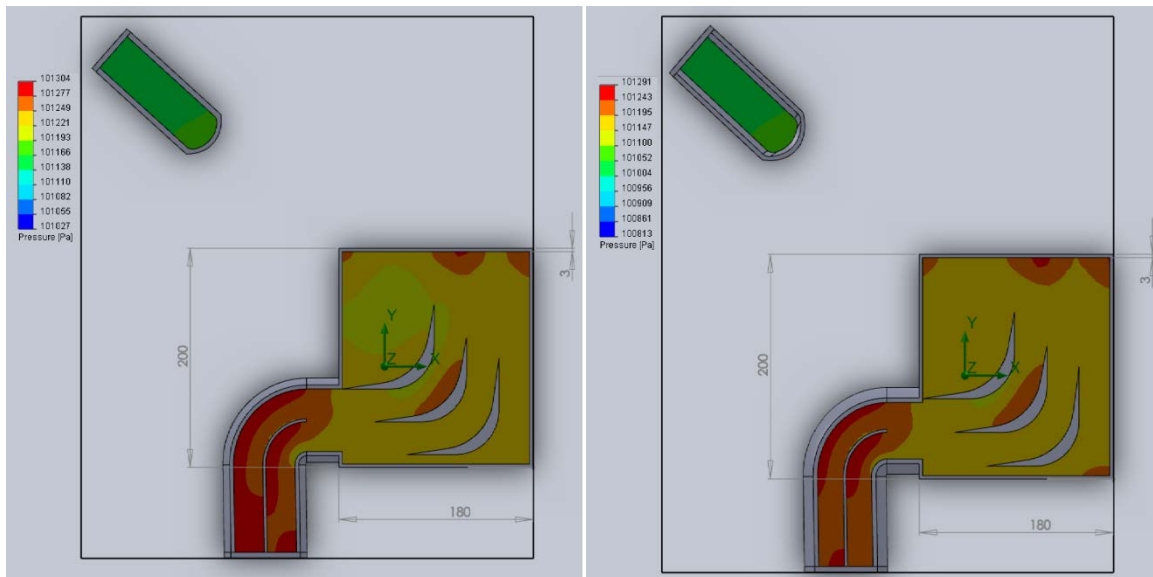
## PRESSURE DISTRIBUTION (WITH GUIDE VANE) AT VARIOUS ENGINE SPEED



1000 r.p.m



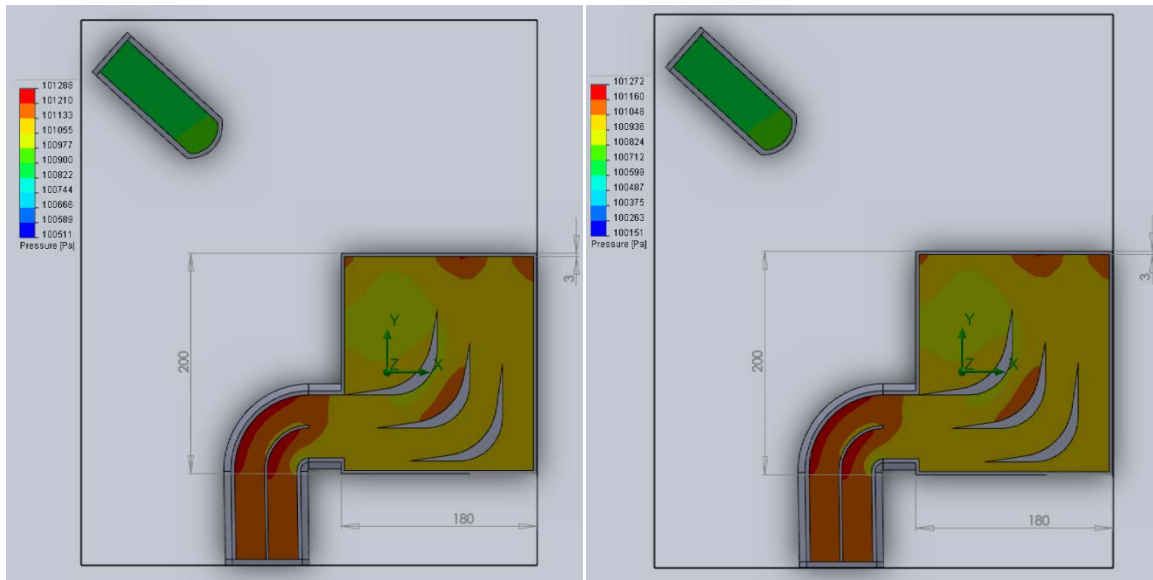
2000 r.p.m



3000 r.p.m



4000 r.p.m

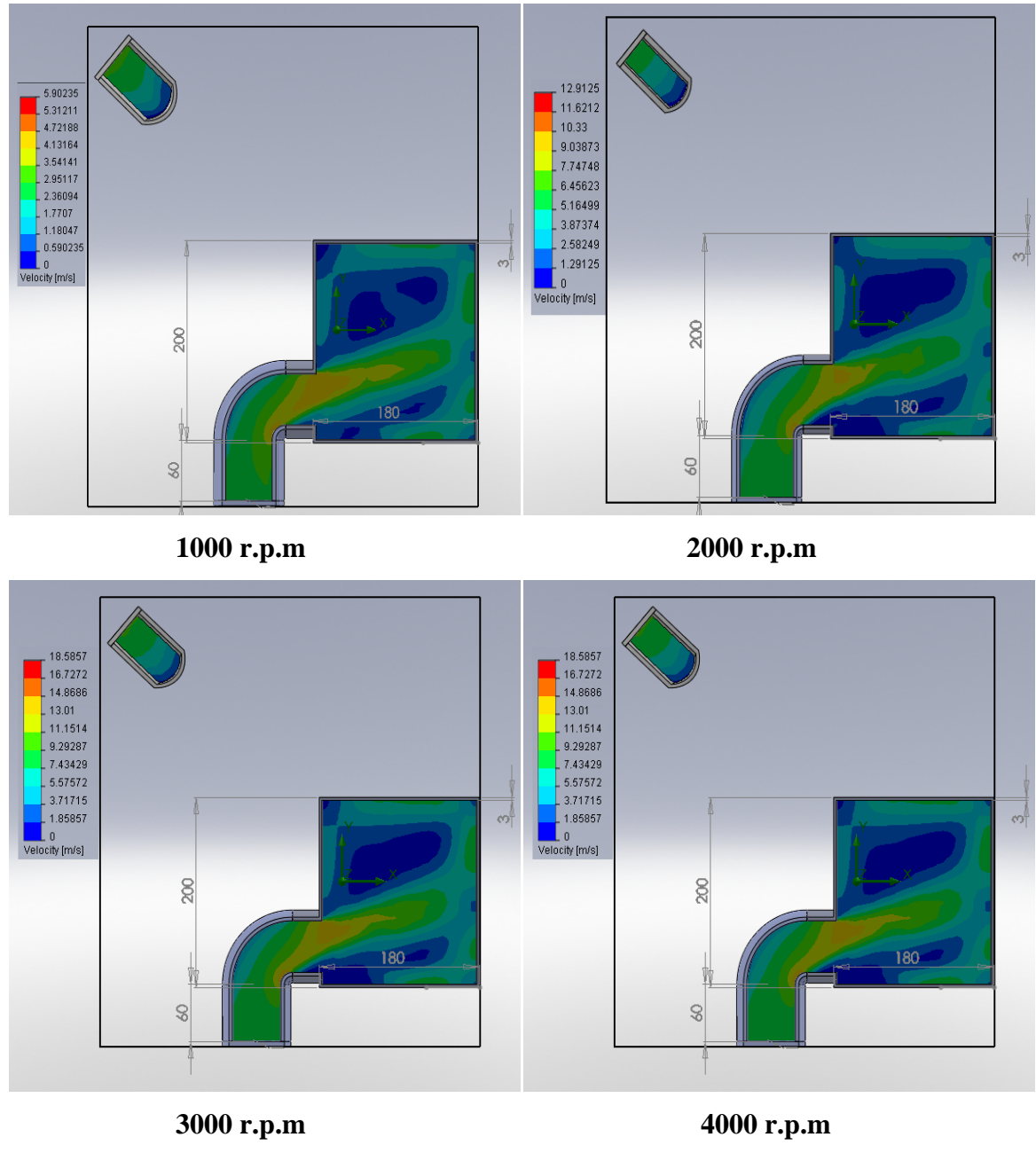


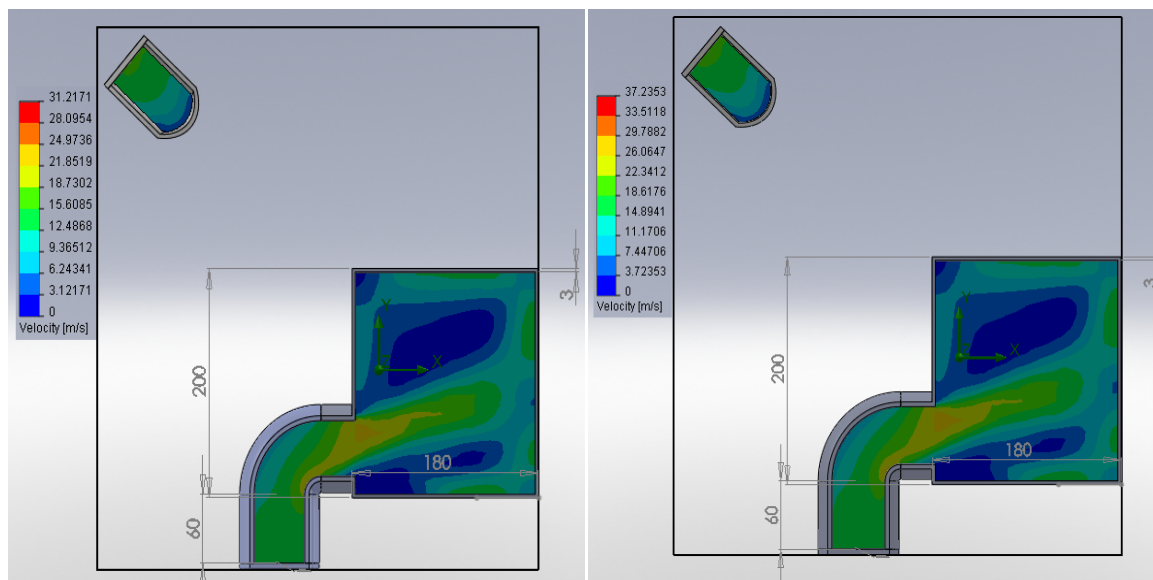
5000 r.p.m

6000 .p.m

**APPENDIX D**

**VELOCITY DISTRIBUTION (WITHOUT GUIDE VANE) AT VARIOUS ENGINE SPEED**



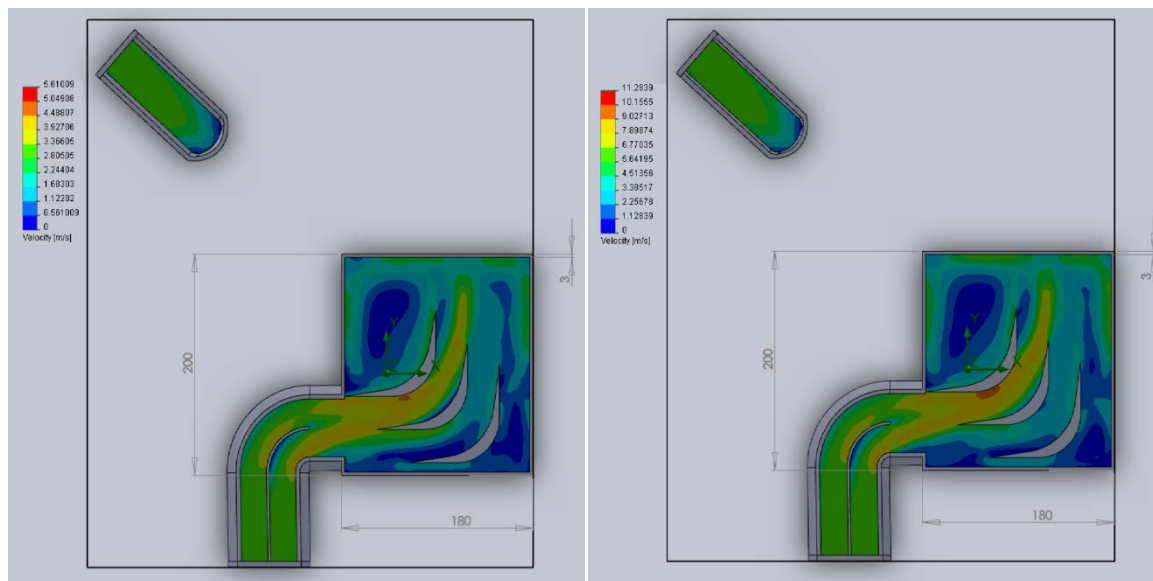


**5000 r.p.m**

**6000 r.p.m**

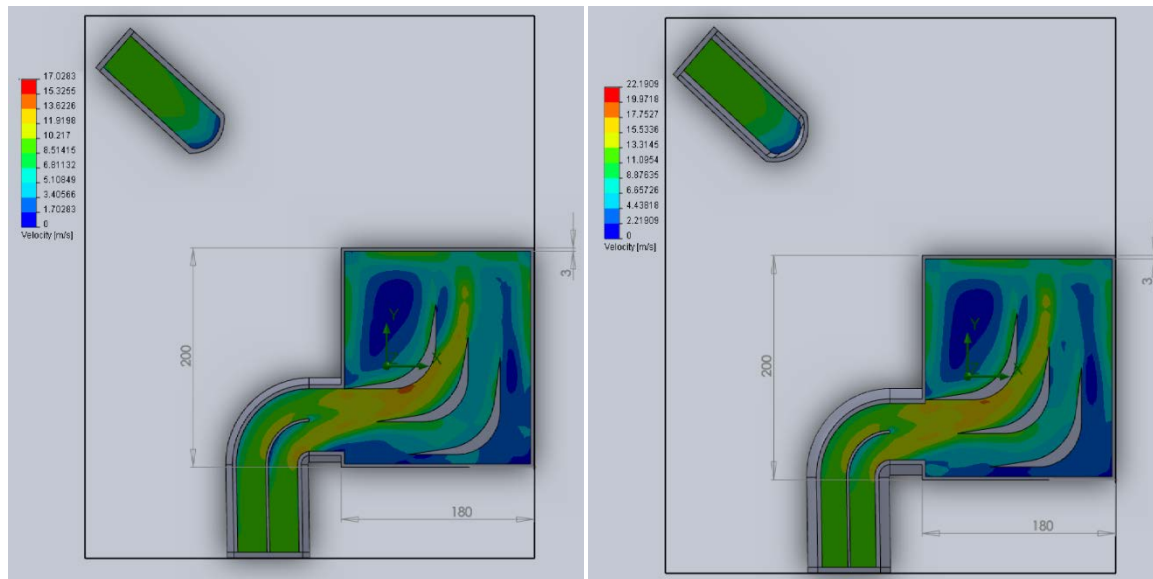
## APPENDIX E

## VELOCITY DISTRIBUTION (WITH GUIDE VANE) AT VARIOUS ENGINE SPEED



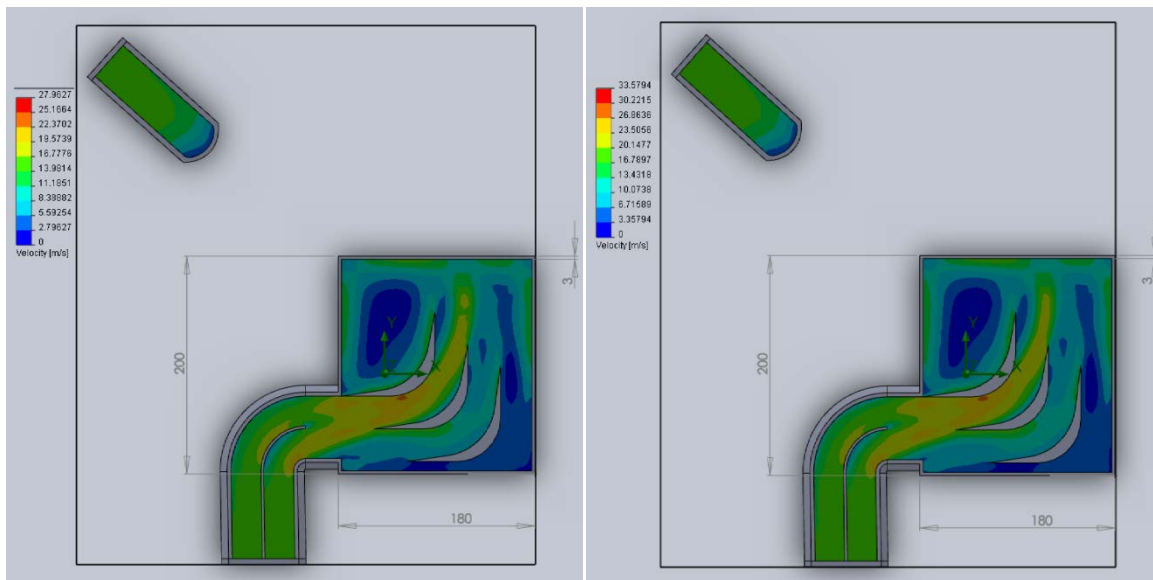
1000 r.p.m

2000 r.p.m



3000 r.p.m

4000 r.p.m



**5000 r.p.m**

**6000 r.p.m**